universität wien

MASTERARBEIT / MASTER'S THESIS

Titel der Masterarbeit / Title of the Master's Thesis

„Construction and characterization of archaeal virus ϕCh1 ORF46(*soj*) and ORF49 deletion mutants"

verfasst von / submitted by

Jana Dragisic, BSc

angestrebter akademischer Grad / in partial fulfilment of the requirements for the degree of

Master of Science (MSc)

Wien, 2017 / Vienna 2017

Studienkennzahl lt. Studienblatt / degree programme code as it appears on the student record sheet:	A 066 834
Studienrichtung lt. Studienblatt / degree programme as it appears on the student record sheet:	Master Molecular Biology
Betreut von / Supervisor:	Ao. Univ.-Prof. Dipl.-Biol. Dr. Angela Witte

Acknowledgements

I would like to express my deepest gratitude to my supervisor Ao. Univ.- Prof. Dipl.- Biol. Dr. Angela Witte for the opportunity to work in her laboratory and her invaluable guidance, patience and suggestions throughout the project, without which this work would not have been possible.

My appreciation also extends to my laboratory colleagues Mikaela Edwards, Richard Manning and Matthias Schmal. A special note of thanks goes to my dear friend Mikaela Edwards for providing me with her support and good humor and Richard Manning for his idea and assistance in creating *soj* deletion mutant.

Above all, my immeasurable thankfulness to my family for their countless encouragement through my journey in college as well as their financial support. And finally, I acknowledge my boyfriend not only for taking the time to comment on this work, but for blessing me with the life of happiness when the lab lights were off.

1. Introduction

1.1. Three domains of life

Over a long period of time prokaryotes were characterized as a single group of organisms whose classification was based on morphology, biochemistry, and metabolism. In 1965, Emile Zuckerkandl and Linus Pauling proposed the idea to use the sequences of different prokaryotes in order to investigate their relations (Zuckerkandl and Pauling, 1965). In 1977, *Archaea* were first distinguished by Carl Woese and George E. Fox as a separate group of prokaryotes (Woese and Fox, 1977). This classification was based on sequences of 16S/18S ribosomal RNA genes which are highly conserved and simple to isolate (Woese and Fox, 1977). Later, Woese proposed a new classification of organisms with three different domains: the Eukarya, the Bacteria and the Archaea (Woese *et al.*, 1990) (Fig. 1).

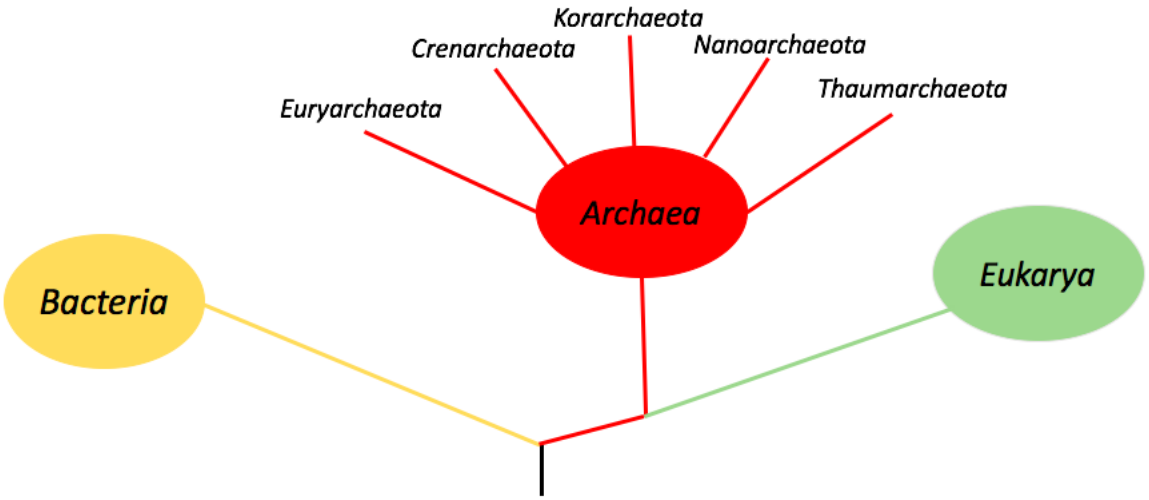

Figure 1. **Schematic representation of three domains of life.** This scheme depicts three domains of life: *Bacteria, Archaea*, and *Eukarya*. *Archaea* consists of five phyla: *Euryarchaeota*, *Crenarchaeota, Korarchaeota*, *Nanoarchaeota,* and *Thaumarchaeota* (Barns *et al*., 1996).

1.2. *Archaea*

Archaea (a greek word meaning “ancient”) constitute one of the three domains of life together with *Bacteria* and *Eukarya*. They are prokaryotes and belong to the group of single-celled organisms. *Archaea* have been first discovered in environments of extreme conditions such as terrestrial hot springs. However, they can also reside with *Bacteria* and *Eukarya* in various highly saline, anaerobic and acidic environments. While the archaeal information processing functions resemble those of *Eukarya*, their core metabolic functions are similar to *Bacteria* (Allers and Mevarech, 2005).

Defined as prokaryotes, archaeal cells lack a cell nucleus and membrane-bound organelles. They exist like spherical, rod shaped, or spiral cells. *Archaea* play an important role in the carbon and nitrogen cycle and there have been indications about their possible involvement in symbiotic fermentation. They often have a commensal life, however, until now, there are no indications of archaeal parasites or pathogens.

Archaea can be divided into two major phyla: the *Euryarchaeota* and the *Crenarchaeota* and three minor phyla: *Korarchaeota*, *Nanoarchaeota,* and *Thaumarchaeota* (Barns *et al*., 1996).

The *Euryarchaeota* can be further divided into eight classes (*Archaeoglobi, Halobacteria, Methanobacteria, Methanococci, Methanomicrobia, Methanopury, Thermococci, Thermoplasmata*), which consist of methanogens, halophiles, thermoacidophiles and hyperthermophiles (Forterre *et al*, 2002). The major part includes the methanogens which are obligate anaerobes and require CO_2 during respiration. The *Halobacteria* contain extremely halophilic species with an optimal growth ranging between 20°C-45°C. The classes *Thermococci* and *Archaeoglobi* are hyperthermophilic *Archaea*. They require marine salt and a neutral pH for their growth.

The *Crenarchaeota* contain only one class, *Thermoprotei* or *Crenarchaeota* with all members being hyperthermophilic and most of them acidophiles. They have been isolated in volcanic habitats and until now, they are the species which require the highest growing temperature in

the range of 60°C to 85°C (Blöchl *et al*., 1997). Considering their metabolic function, they range from chemolithoautotrophic to chemoorganotrophic.

The three minor phyla could not be isolated under laboratory conditions until now. Therefore, all available studies are based on molecular sequences (Brochier-Armanet *et al*., 2011; Huber *et al*., 2002; Barns *et al*., 1996). However, in 2008, a new ammonia-oxidizing *Archaeon* was discovered and classified as member of the phylum *Thaumarchaeota* that supposedly separated before division of *Crenarchaeota* and Euryarchaeota (Pester *et al*., 2011). Subsequent analysis showed that *Thaumarchaeota* are indeed distinguishable from other archaeal species. Organisms classified as *Thaumarchaeota* are chemolithoautotrophic ammonia-oxidizers and play an important role in the ammonium and carbon cycle (Spang *et al*., 2010).

1.2.1. Archaeal features

Archaea display various unique characteristics that are not found in the other two domains of life. However, there are certain archaeal features that rather resemble Bacteria while other characteristics share similarities with *Eukarya*.

Evolution of archaeal cell wall enabled survival under extreme conditions (Gribaldo *et al*., 2006). A semi-rigid layer providing the balance and shape to the cell is observable in almost all archaeal cells. The majority of *Achaea* contain a cell wall composed of pseudopeptidoglycan (pseudomurein) which provides the cell with structural integrity and counteracts the osmotic pressure from the cell's cytoplasm. The pseudopeptidoglycan consists of L-N-acetyltalosaminuronic acid with a β-1,3 linkage to D-N-acetylglucosamine; the amino acid interbridge lacks D-amino acids (Albers and Meyer, 2011). One of the most abundant protein is the surface layer (S-layer) which is anchored to the cytoplasmic membrane (Jarrell *et al*., 2011). S-layer can form a two-dimensional crystalline protein or glycoprotein consisting of two, three, four, or six subunits (Klingl, 2014) (Fig. 2).

Another component that distinguishes *Archaea* from other domains is the polymer methanochondroitin which is utilized for the formation of the cell wall or it can supported by an additional S-layer (Albers and Meyer, 2011).

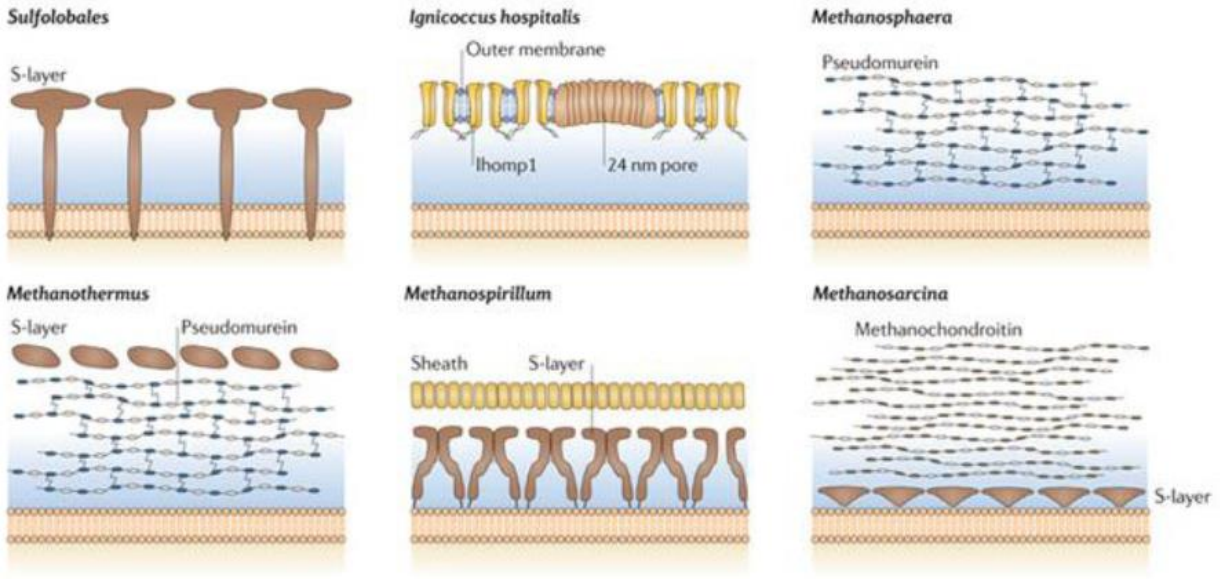

Figure 2. Major types of archaeal cell walls. The major type of archaeal cell wall is S-layer composed of either glycoprotein or protein. *Ignicoccus hospitalis* and *Methanosphera* do not possess S-layer. However, *Ignicoccus hospitalis* contains an outer membrane. Additionally, there are two other polymers present in *Archaea*: pseudomurein or methanochondroitin (Albers and Meyer, 2011).

A major difference between *Archaea* and the other two domains of life is the composition of membrane lipids. In *Archaea*, the membrane lipids consist of ether-linked branched isoprenoid chains whereas in *Bacteria* and *Eukarya*, there are ester-linked unbranched fatty acids (Albers and Meyer, 2011) (Fig. 3). The ether-linked branched membrane lipids are more resistant to higher temperatures, oxidation, and enzymatic degradation by phospholipases (van de Vossenberg *et al*., 1998). Therefore, some *Archaea* are more stable due to these larger hydrophobic chains that span through the whole membrane and are linked to the glycerol backbone. The majority of extreme halophilic Archaea exhibit a ubiquitous phospholipid called archaetidylglycerol methylphosphate (PGP-Me) which is used to construct polar membrane

lipids. The previous studies demonstrated that the membrane's stability in high salt concentrated environments is due the PGP-Me (Tenchov *et al*., 2006).

In general, it has been proved that archaeal membranes seem to be more stable and rigid as well as more tolerant to the high salt concentrations, thus facilitating the life in extreme environments (van de Vossenberg *et al*., 1998).

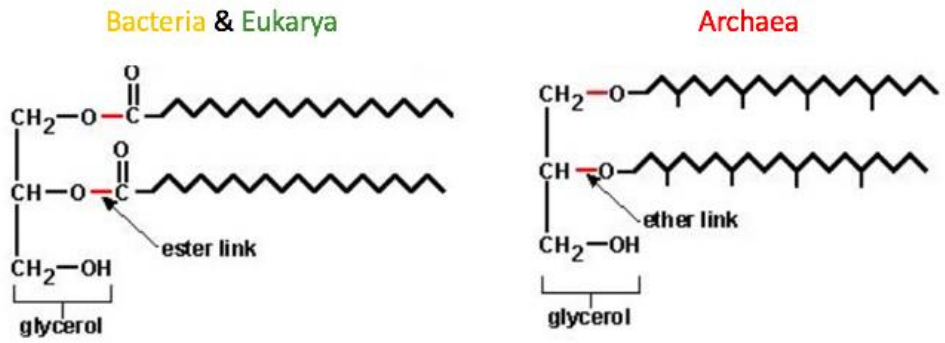

Figure 3. Membrane lipids of *Bacteria*, *Eukarya* and *Archaea*. In *Archaea* branched isoprens are ether linked to a sn-glycerol-1-phosphat moiety, whereas in *Bacteria* and *Eukaryotes* the glycerol moiety is ester linked to a sn-glycerol-3-phosphate backbone (adapted from Kaiser, 2017).

1.2.2. Halophilic and haloalkaliphilic *Archaea*

Halophilic organisms are capable of living in high salt environments. Their habitats include e.g. hypersaline lakes in Africa or the Dead Sea, whose salt concentrations are higher than those of the oceans due to higher evaporation rates (Oren, 2002). Halophiles can be classified as halotolerant, moderate halophile, and extreme halophile depending on their salt tolerance. Halotolerants tolerate high salt concentrations whereas the moderate halophiles grow in media with a salt concentration ranging from 0.5 M to 2.5 M NaCl. Extreme halophilic *Archaea* require concentrations of 2.5 M to 5.2 M NaCl for their optimal growth (Andrei *et al*., 2012). The halophilic Archaea had to evolve in order to adapt to the life in extreme conditions.

Haloalkaliphilic organisms are adapted to the environments with high salt and alkaline conditions. Many hypersaline lakes have a reddish-purple color which comes from a α-

bacterioruberin (a 50 carbon carotenoid pigment) and its derivatives present in the membranes of archaea from the *Halobacteriaceae* family that belongs to the phylum *Euryarchaeota* (Shahmohammadi *et al*., 1998). Due to a high exposure to the sun and high amounts of UV radiation in salt ponds, the *Halobacteriaceae* developed a new mechanism for DNA repair. The bacterioruberin plays a primary role in protecting the DNA by serving as an antioxidant and assuring the protection against reactive oxygen species.

1.2.2.1. Adaptations to high salt environments

As previously mentioned, the halophilic and haloalkaliphilic *Archaea* experienced various adaptations to be able to tolerate high salt concentrations. There are two different strategies to deal with osmotic pressure. The first strategy is "salt in" which is used by extremely halophilic organisms. This approach is based on the accumulation of potassium chloride in the cell and effective pumping out of sodium ions via Na+/H+ antiporter systems. These organisms are able to thrive in media with salt concentration ranging between 3-4 M KCl or NaCl (Fendrihan *et al*., 2006). In addition, other studies have shown that one of the molecular adaptions includes the presence of more acidic amino acids in the proteins' structure (Oren, 1999).

Other halophilic and halotolerant *Archaea* use another strategy called "compatible solute strategy". They thrive in environments with small salt concentration and take up the solutes such as glycerol, amino acids, and sugars to balance the osmotic potential (Oren, 1999). This approach requires more energy in comparison to the "salt-in" strategy.

In addition to the high salt, the haloalkaliphilic *Archaea* require a pH ranging between 8 and 11 as well as low Mg^{2+} concentration. Since most enzymes require a neutral pH for their functionality, the intracellular pH has to remain neutral which is enabled by the Na+/H+ antiporter system.

1.2.2.2. Halophilic and haloalkaliphilic proteins

Parallel to cell membranes, the halophilic proteins had to adapt in order to survive harsh conditions. Their surface consists of acidic residues, such as aspartic and glutamic acids and of less hydrophobic amino acids (Tadeo *et al*., 2009). The acidic amino acids help to maintain the excess of protein hydration and keep the surface flexible (Nayek *et al*., 2014).

Additionally, it has been shown that the haloalkaliphilic proteins developed mechanisms to maintain a neutral pH in their cytoplasm via glycosylated proteins. It was observed that the protein composition in haloalkaliphilic *Archaea* is similar to halophilic *Archaea*. In both groups the majority of amino acids are acidic (Reed *et al*., 2013).

In general, the halophilic proteins show activity at low water availability and thrive well at high salt concentrations (Allers, 2010).

Furthermore, controlled gene expression is very important for the investigation of protein functions. In order to turn a certain gene on or off, there has to be an inducible promoter. Various promoters have been found for Archaea, such as Pr bop which comes from the bacterioopsin gene and can be induced by high-light intensities and low-oxygen levels (Patenge *et al*., 2000). Another example is the ferredoxin promoter (Pfdx) from the ferredoxin gene that codes for ferredoxin in *H. salinarum* (Gregor and Pfeifer, 2005). In 2007, a promoter from the tryptophane gene was isolated which is strongly induced in the presence of tryptophane (Large *et al*., 2007). Kixmüller and Greie discovered the kdp promoter (Pkdp) of *H. salinarum* in 2012 which is dependent on the K+ concentration. The lower the K+ concentration, the higher the expression of the kdp promoter.

Very few archaeal expression systems are available to date. However, future establishments of such systems are essential for better understanding of *Archaea* and their potential roles.

1.2.3. Biotechnological Applications of *Archaea*

In the last years, *Archaea* have been subject of many studies due to their industrial applications. Halophilic *Archaea* are important for bioremediation, degradation of organic pollutants, and in wastewater treatment processes (Margesin and Schinner, 2001).

Apart from uses of archaeal biomasses, archaeal enzymes have a wide range of possibilities for industrial applications. The enzymes derived from thermophilic *Archaea* show stability in organic solvents whereas acidophilic *Archaea* display a potential use in mineral processing. (Norris *et al*., 2000). In addition, conversion of starch to *e.g.* dextrins, glucose, or fructose is achievable through their thermostable enzymes. Other enzymes isolated from *Archaea* that degrade polymers such as cellulases and xylanases can be utilized in the pharmaceutical, paper, and waste treatment industries. Additionally, hyperthermophilic proteases are used as degrading agents in detergents (Schumacher *et al*., 2001).

Some archaeal proteins and special lipids have potential biotechnological applications. For instance, the retinal pigments bacteriorhodopsin and halorhodopsin that are bound to the membrane allow microorganisms to use light energy to drive bioenergetic processes (Oren 2002; Janos K. Lanyi, 1995). Additionally, halophilic *Archaea* produce osmotically active substances called “compatible solutes” that are shown to be excellent stabilizers for biomolecules (da Costa *et al*., 1998) and are used as moisturizers in cosmetics or as stabilizers in polymerase chain reaction (Sauer and Galinski, 1998). Furthermore, liposomes formed from unique archaeal lipids are very stable and might serve as an alternative for delivering drugs into the body (Gambacorta *et al*., 1995).

Several new antibiotics were discovered by using alkaline media to isolate new microorganisms. They could be of high importance due to their different structure in comparison to bacterial antibiotics. However, none of these antibiotics are yet commercially available. Some of the reasons are their low stability under alkaline conditions, low expression levels of proteins and metabolites as well as difficulties in purification processes (Schiraldi *et al*.,2002).

In conclusion, *Archaea* play an important role in various biotechnological processes. It is expected that future research will significantly increase the range of applications in industry and health sciences.

1.2.4. *Natrialba magadii*

Natrialba magadii, a haloalkaliphilic archaeon belonging to the family of *Halobacteriaceae* within the phylum Euryarchaeota, was first isolated in 1984 from the soda lake Magadi in Kenya by Tindal *et al*. (1984). Lake Magadi is an extremely saline and alkaline lake. The lake contains high levels of carbonates, salt concentration up to 300 g/L, and a pH exceeding 11 (Aharon Oren 2002; Ma et al. 2010) Mg^{2+} and Ca^{2+} are undetectable due to their precipitation in the presence of high pH. Magadi is renewed by saline hot springs whose temperature can reach 86°C.

When first discovered, *N. magadii* was classified as part of the genus *Natronobacterium,* called *Natronobacterium magadii*. However, sequencing the 16S rRNA and comparison with other species of *Natronobacterium* led to a new genus *Natrialba* and thus the original *Natronobacterium magadii* was given a new name - *Natrialba magadii* (Kamekura *et al*., 1997).

Since *N. magadii* is a haloalkaliphilic organism, it requires a rich medium containing 3.5-4 M of sodium chloride and a pH between 9.5 and 11. Salt concentrations below 1.5 M NaCl cause higher osmotic pressure and lead to lysis. In addition, *N. magadii* needs temperature ranging from 37°C to 42°C for its optimal growth. It is strictly aerobic and a chemoorganotroph organism that obtains its energy from the oxidation of organic compounds. It grows proteolytically, therefore, it is essential to supply the medium with amino acids and peptides which are then used as carbon and energy source.

N. magadii cells are rod-shaped cells with a reddish color due to carotenoid pigments present in their membrane. They have length of 5-7 μm (Tindall *et al*., 1984). Motility is achieved through polar flagella. It is a polyploid organism that contains up to 50 copies of chromosomal DNA per cell. Therefore, its generation time is approximately 9 hours, thus being significantly longer than

the generation time of *E. coli* (20 minutes). Another explanation for longer generation time are the environmental extremes in which haloalkaliphilic *Archaea* thrive.

1.2.4.1. *N. magadii* under laboratory conditions

1.2.4.1.1. Transformation

The first successful transformation of *Archaea* was accomplished in 1987 by Cline (Cline and Doolittle, 1987). They used spheroplast transfection based on polyethylene glycol in order to transform ϕH DNA into extremely halophilic *Halobacterium halobium*. The transformation efficiency was analyzed via plaque assay. This approach is based on removal of S-layer by using EDTA which triggered the formation of spheroplasts. However, EDTA was shown not to be sufficient for removal of *N. magadii's* S-layer. Therefore, *N. magadii* cells were treated with bacitracin which prevents glycosylation of S-layer and proteinase K. This method led to generation of spheroplasts which were able to take up foreign DNA (Mayrhofer-Iro *et al*., 2013). (Fig. 4). Subsequently, they were incubated at 37°C to regenerate. Despite lower transformation efficiency, this approach represents the first successful transformation into the haloalkaliphilic archaeon *N. magadii*.

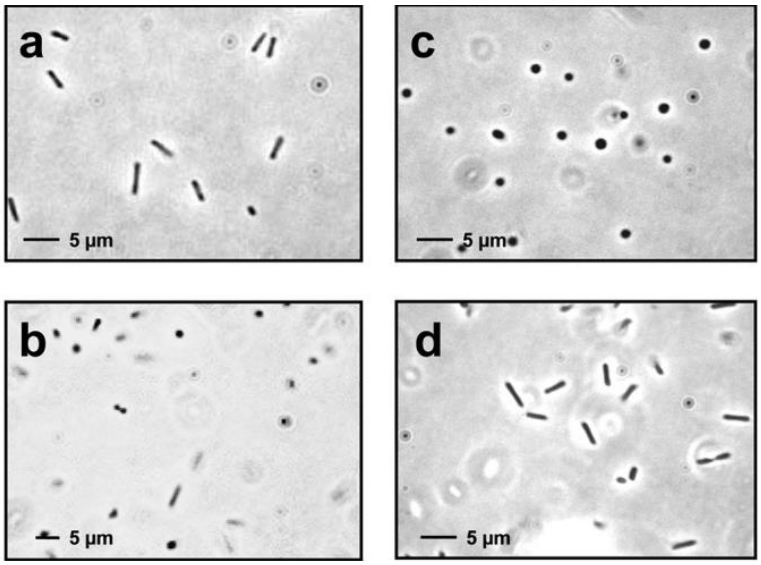

Figure 4. Preparation of *N. magadii* competent cells. The *N. magadii* cells were grown in rich medium (a) and in the presence of bacitracin (b). After incubation with proteinase K at 42°C for 48 hours, competent cells were transformed (c). Cells were regenerated for 48 h at 37°C in rich medium (d) (Mayrhofer-Iro *et al*., 2013).

1.2.4.1.2. Shuttle vectors and selectable markers

It is of crucial importance to create different shuttle vectors in order to genetically manipulate *Archaea* and study their functions.

There are only two available antibiotics which serve as selection markers: novobiocin and mevinolin. Novobiocin inhibits bacterial DNA gyrase by blocking the ATP-binding site (Holmes and Dyall-Smith, 1991). Additionally, it has been proven that novobiocin is involved in inhibition of cell growth and altering the supercoiling of plasmids (Holmes and Dyall-Smith, 1990). Another crucial marker is mevinolin that inhibits HMG-GoA (3-hydroxy-3methylglutaryl-coenzym A) reductase which is necessary for the synthesis of isoprenoids and thus for formation of archaeal membranes (Lam and Doolittle, 1992).

Up to this point, there are two frequently used shuttle vectors: pRo-5 and pNB102 (Fig. 5). Two other vectors, pNBRM1 and pNBRM2 (Manning, 2017), were described in 2017, but have only been utilized rarely.

pRo-5 contains the vector pKSII+ and contains an origin of replication and ampicillin resistance (*bla*) as a selection marker for cloning in *E. coli*. Additionally, a novobiocin resistance gene can be found on the plasmid encoding a mutated *gyr*B gene isolated from *Haloferax alicantei* and can serve as a selection marker for cloning into *N. magadii* (Mayrhofer-Iro *et al*., 2013). Furthermore, parts of ORF53 and ORF54 can also be found on the plasmid which are essential for autonomous replication in *N. magadii* (Mayrhofer-Iro *et al*., 2013). According to multiple studies pRo-5 yields the highest transformation efficiency among all tested pRo vectors (Mayrhofer-Iro *et al*., 2013).

The shuttle vector pNB102 is constructed from the cryptic plasmid pNB101 and contains ColE1 origin of replication of E. coli as well as resistance for ampicillin and mevinolin (Zhou *et al*., 2004).

A **B**

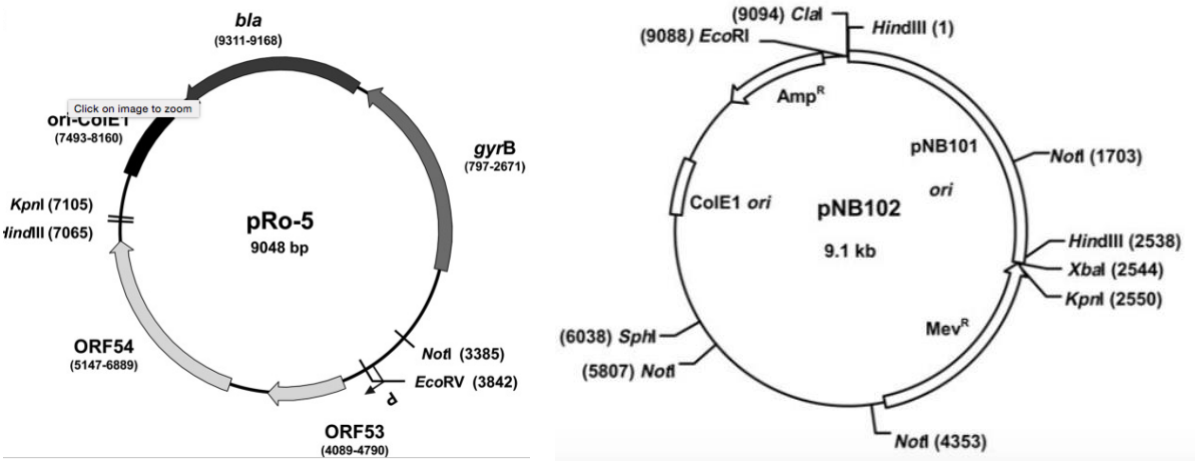

Figure 5. Schematic representation of shuttle vectors for *N. magadii*. Both shuttle vectors can be used for *E. coli* and *N. magadii*. A) pRo-5 vector has ampicillin resistance for *E. coli* and novobiocin for *N. magadii* B) pNB102 vector contains resistance against ampicillin for *E. coli* and mevinolin for *N. magadii* (Mayrhofer-Iro *et al*., 2013; Zhou *et al*., 2004).

1.2.4.1.3. *N. magadii* L11 and *N. magadii* L13- available laboratory strains

N. magadii strains L11 and L13 are available and used in laboratory so far. The strain *N. magadii* L11 is lysogenic and harbors ϕCh1 that is integrated into the host's genome and coexists as a provirus. Spontaneous lysis of the lysogenic strain *N. magadii* could be observed as the culture entered the stationary phase. Virus particles were detected in the supernatant of the culture (Witte *et al*., 1997). To our knowledge, there are no other hosts of ϕCh1 other than *N. magadii*. The second strain named *N. magadii* L13 is cured of virus by passaging many times of the *N. magadii* L11 culture. However, re-infection is possible. Figure 6 represents the electron micrographs of the laboratory strains *N. magadii* L11 and *N. magadii* L13.

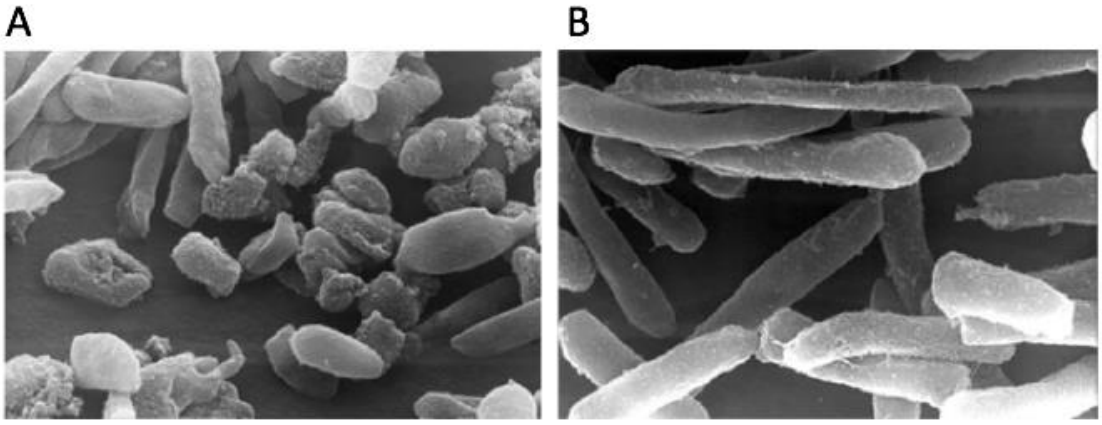

Figure 6. Electron micrographs of *N. magadii* strain L11 and *N. magadii* L13. A) *N. magadii* strain carrying ϕCh1 as a provirus. B) L13 strain lacking the ϕCh1 virus (Iro *et al*., 2007).

1.3. Archaeal viruses

Despite the fact that *Archaea* resemble *Bacteria* in cellular and genome organization, archaeal viruses differ from DNA viruses of *Bacteria* and *Eukarya*. Recent studies reported that a head-tail morphology, which resembles bacteriophage structure is rare among archaeal viruses. Archaeal viruses contain mostly double stranded DNA and only one virus has been identified to possess a single stranded DNA called Aeropyrum coil-shaped virus (ACV) (Happonen *et al*., 2010). DNA genomes are either linear or circular and range in size from 12-230 kbp (Snyder *et*

al., 2003). Up until now, no studies discovered RNA archaeal viruses (Mochizuki *et al*., 2012). As a matter of fact, archaeal viruses that contain dsDNA genome show various morphotypes such as fusiform, linear, bottle-shaped, and droplet-shaped viruses, spherical, and combinations of these features. (Dyall-Smith *et al*., 2003).

Fusiform viruses are exclusive to hyperthermophiles, extreme halophiles and anaerobic methane-producers from the *Euryarchaeota* and *Crenarchaeota* which inhabit hot, acidic, and hypersaline waters (Rice *et al*., 2001; Oren *et al*., 1997).

The most remarkable example of bottle-shaped viruses is *Acidianus* bottle-shaped virus (ABV). As the name suggests, its structure resembles a bottle and infects the hyperthermophilic *Acidianus* genus. Basic architecture differs from any known virus and absorption to the host cell seems to happen through its narrow end.

The virus (SNDV) infecting *Sulfolobus neozealandicus* represents a droplet-shaped virion which dsDNA genome seems to be modified. However, it has not been sequenced yet.

Linear viruses predominate in hot terrestrial environments with temperatures of above 80°C. All isolated viruses infect the genera *Sulfolobus, Acidianus* and *Thermoproteus*. For the first time is was observed that linear viruses possess dsDNA genomes. In contrast to other archaeal viral families, a substantial part of orthologous genes encoding glycosyl transferases and transcriptional regulators, are shared by linear viruses.

Spherical viruses exhibit two main types: *Pyrobaculum* spherical virus (PSV) which is enveloped and *Thermoproteus tenax* spherical virus 1 (TTSV1). Other two known spherical viruses are *Sulfolobus* turreted icosahedral virus (STIV) and *Haloarcula hispanica* virus (SH1) displaying non-tailed icosahedra with an internal lipid bilayer (Prangishvili *et al*., 2006).

In addition to the icosahedral viruses, head-tail viruses can be frequently found in *Archaea*. They are non-enveloped virions carrying icosahedral heads and helical tails. Sixteen head-tail viruses have been reported which are associated with the *Euryarchaeota*. These viruses particularly infect extreme halophiles or methanogens. They have been assigned to the families *Myoviridae* and *Siphoviridae*, respectively. In addition to the phage-like structure, their genome

content resembles dsDNA bacteriophages. The best characterized myoviruses are ϕh infecting the *Halobacterium salinarum* and ϕCh1 infecting *Natrialba magadii*. Another two well studied haloarchaeal viruses are HF1 and HF2 which are reported to be the first lytic viruses and infect *Halobacterium, Haloarcula, Haloferax, Halorubrum,* and *Natrialba* (Dyall-Smith *et al*., 2003). Here, we investigated the haloalkaliphilic virus ϕCh1.

1.3.1. Haloarchaeal viruses

1.3.1.1. ϕCh1 virus

In 1997, investigating a haloalkaliphilic archaeon *N. magadii Witte et al.* observed a spontaneous lysis of *N. magadii* in stationary cultures, which later led to the discovery of a temperate virus called ϕCh1. This virus is the first described virus that infects haloalkalophilic archaeon *N. magadii.* It has been observed that re-infection was not feasible. Therefore, after subculturing and testing for infection with ϕCh1, a cured strain named L13 was obtained, which could be infected again. A lysogenic strain, named L11, was obtained after inoculating a single plaque formed by a virus (Witte *et al*., 1997).

ϕCh1 belongs to the family of *Myoviridae* and considering its morphological features resembles the phage ϕH of *H. salinarum* (Schnabel and Zillig, 1984). Inspection of electron micrographs revealed the virus' morphology, showing its head-tail structure. The total length is determined to be app. 200 nm with a length of 70 nm for head and 130 nm for tail. The width is 20nm (Fig. 7). Structures at the end of the tail are considered important for adsorption (Fig. 8).

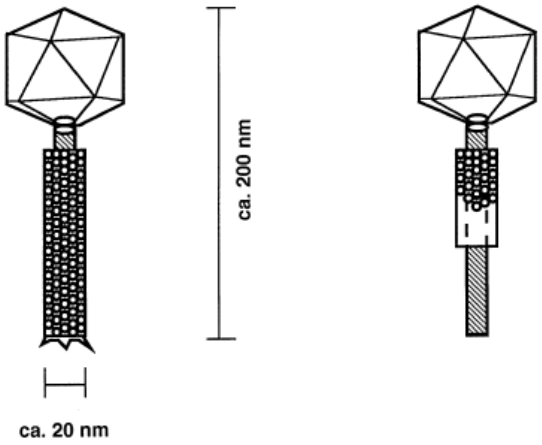

Figure 7. Schematic representation of ϕCh1 particles and its dimensions. The total length of ϕCh1 is app. 200 nm whereas its width is determined to be 20 nm (Witte *et al.*, 1997).

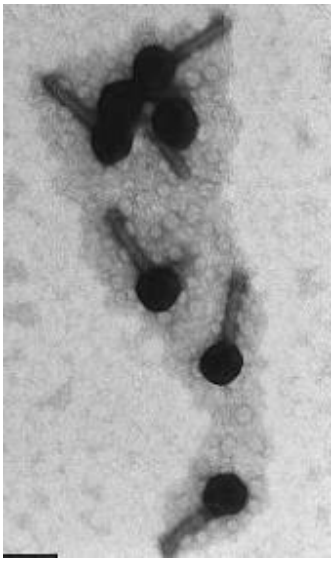

Figure 8. Electron micrographs of ϕCh1 particles negatively stained with uranyl acetate (Witte *et al.*, 1997).

It has been shown that salt concentration plays an important role for ϕCh1 infectivity and stability. Loss of infectivity was observed below 2 M NaCl suggesting either conformational changes of the capsid proteins or dissociation of virus particles. There are at least four major (A, E, H, and I) and five minor (B, C, D, F, and G) proteins with molecular masses ranging from 15 to

80 kDa as shown by SDS-PAGE analysis. All proteins were determined to be acidic with isoelectric points between pH 3.3 and pH 5.2 as already shown for a number of proteins from halophilic *Archaea* (J K Lanyi, 1974).

ϕCh1 has a unique genome organization. It exists as a chromosomally integrated provirus and contains a linear double-stranded DNA (app. 55 kbp) as well as RNA that seems to be packaged in the mature phage particle of ϕCh1. There are at least eight different RNAs so far known and the ratio to DNA is 5:1. The origin of RNA is still not clear. However, it is assumed that it is rather host specific than encoded by the virus itself and is shown to be unaccessible to RNase A degradation.

It has been suggested that ϕCh1 is a temperate virus. Upon infection, the virus can switch between two different pathways: the lytic and the lysogenic. In the lytic cycle, the viral DNA floats freely, replicates separately from the host DNA and leads to cell lysis. In the lysogenic cycle, it gets integrated into the host genome with the help of site-specific recombinases (Landy, 1989). As previously mentioned, after spontaneous lysis of *N. magadii* culture, the ϕCh1 particles were collected. Southern Blot analysis showed that ϕCh1 can be integrated into a chromosomal DNA, suggesting it to be a provirus. Additionally, the ϕCh1‘s episomal state has also been observed (data not shown). There are indications that either Int1 or Int2, which code for putative site-specific recombinases of the bacteriophage lambda integrase type might have a function in integration of viral genome into the host genome. Pal1 to Pal4 sequences might also be involved into this process. Additional roles of pal1 and pal4 might include regulation of gene expression by inversion of DNA fragments or decatenation of ϕCh1 plasmids by recombination between pal sites to ease partition of plasmids to daughter cells (Hallet and Sherratt, 1997).

The partial resistance to the restriction of ϕCh1 DNA by *Eco*RV suggested modification of some bases. Further experiments revealed the presence of two fractions of ϕCh1 DNA: one which is methylated at Dam-like sites and the other being non-methylated. Restriction fragments of intermediate length do not occur, indicating that there are no hemimethylated sites. The data

showed that adenine residents appeared to be methylated. This was surprising since the *N. magadii* DNA was not Dam-methylated (David Lodwick *et al*., 1986).

The nucleotide sequence of ϕCh1 was first completely determined in 2002 by Klein *et al*., identifying 98 different open reading frames (ORFs) (Fig. 9). The genome consists of 58 498 bp with a G+C content of 61.9%.

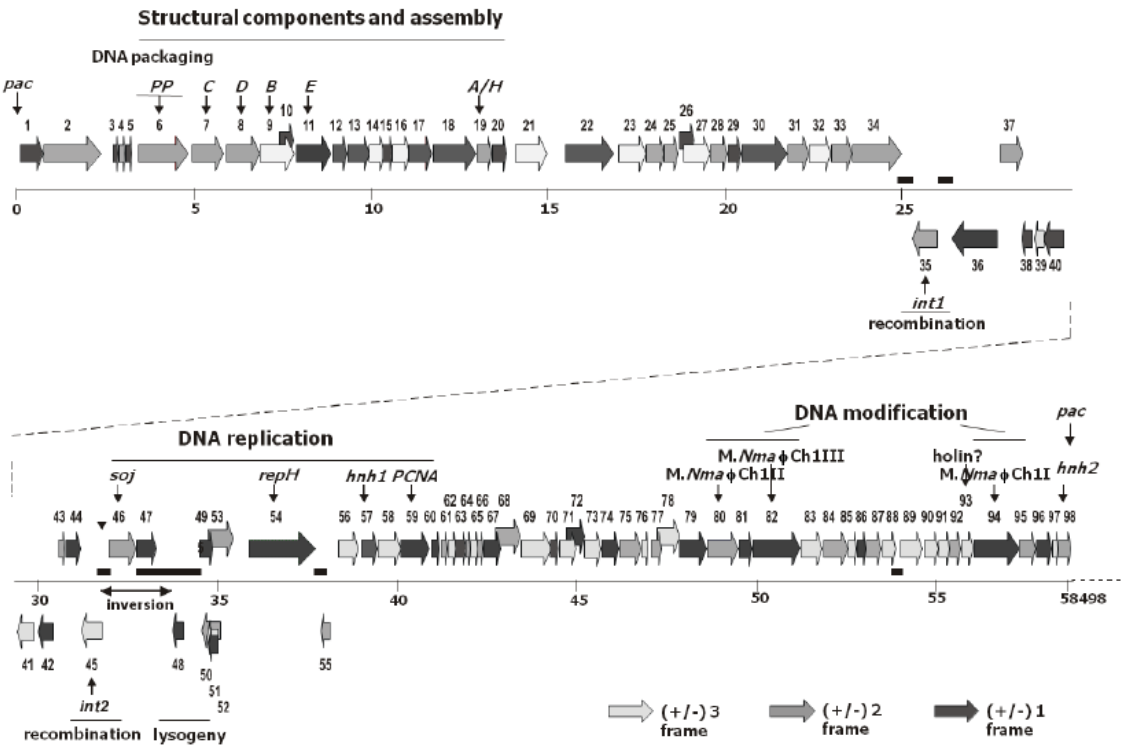

Figure 9. Representation of ϕCh1 genome.

58 498 bp of virus ϕCh1 are represented together with 98 ORFs marked by arrows. The genome consists of three parts: i) the left part consisting of genes coding for structural proteins and probably involved in virion morphogenesis, ii) a central part being important for replication, regulation of gene expression and plasmid stabilization and iii) the third part comprises mostly genes of unknown function and genes coding for DNA methylation and restriction (Klein *et al*., 2002).

Most of the ORFs start with ATG and only four ORFs (3, 41, 79 and 83) start with GTG. The overall codon usage has been determined using 14 ORFs (6, 11, 18, 19, 35, 40,45,46, 48, 54, 59,

80, 82, and 94). G and C are usually found in the wobble position showing the similarity to that of halophilic *Archaea* (Klein *et al*., 2002).

The ϕCh1 genome can be divided in three parts: i) the left part consisting of genes (ORFs 1-34), which are rightward-transcribed, code for structural proteins and are probably involved in virion morphogenesis, ii) a middle part (ORFs 35-55), which are left- and right-transcribed, being important for replication, regulation of gene expression and plasmid stabilization and iii) the third part comprises mostly genes (ORFs 56-98) of unknown function and genes coding for DNA methylation and restriction (Fig. 9). Arrangement of ORFs indicate formation of transcriptional units. Homology searches revealed that only 48 ORFs matched other known sequences, out of which 17 were similar to the proteins with already known function. A comparison of the ϕCh1 genome with the ϕH led to the conclusion that the central part of ϕCh1 is highly similar to the so-called L-segment (pϕHL), which can circularize and replicate on its own. The similarity varies between 50% and 97% over the entire length of the sequences. Interestingly, the entire ORFs or parts of ORFs that are similar to the members of HNH family of endonucleases are different between ϕCh1 and ϕH, e.g. the HNH domain of ORF47 is lacking in ϕCh1 whereas it has been found in ϕH. However, the main difference between ϕH and ϕCh1 is lack of insertion sequences (IS) in the ϕCh1. *H. salinarum*, the host of ϕH requires a neutral pH for its growth and harbors plenty of distinctive sequences which might explain the presence of different IS elements. However, studies showed that ϕCh1 cannot infect *H. salinarum* cells or is incompetent of producing progeny and thus does not include *H. salinarum* as a host. (Schnabel and Zillig 1984). The overall genome organization of ϕCh1 is documented for many tailed bacteriophages (Casjens *et al*., 1992; Brüssow and Desiere, 2001). The architecture of archaeal head-tail viruses is conserved across the domains of life due to either a common ancestor of tailed dsDNA viruses of *Bacteria* and *Archaea* or horizontal gene transfer.

When restricted, a DNA isolated from the lysogenic strain *N. magadii* L11 showed a circular replicative form of the virus DNA. Several proteins have been identified to be involved in plasmid replication and stabilization. Among those proteins are RepH, Int1, and Int2, which

have been shown to be site-specific recombinases and the putative binding sites pal1 to pal4 that might be involved in plasmid separation as well as Soj.

ϕCh1 virus does not encode its own DNA polymerase as seen in BLAST analyses. However, it has been shown that the virus possesses a homologue of eukaryal and archaeal proliferating cell nuclear antigen (PCNA) which is induced by p53 gene and is essential for determining the cell's fate. In the absence of p53 and presence of PCNA, DNA replication and repair occur. When PCNA is present in lower amount or is lacking, the apoptosis takes place (Paunesku *et al*., 2001). A potential role of PCNA may be in binding DNA polymerases, which are encoded by *N. magadii*. The study from 2000 showed that PCNA might also interact with the ϕCh1-encoded methyltransferase M.ϕCh1 (Baranyi *et al*., 2000).

1.3.1.1.1. ORF46 (*soj*)

The Soj protein is encoded by ORF46 of ϕCh. Studies showed that *Soj* is involved in plasmid and chromosomal partitioning. Plasmids are extra-chromosomal pieces of DNA that can self-replicate and assist in adaptation of their hosts to specific niches through the expression of selected genes (Boucher *et al*., 2013; Heuer and Smalla, 2012; Leplae *et al*., 2006). As plasmids represent a metabolic burden for their hosts, mechanisms ensuring plasmid transmission to daughter cells are essential for their stable maintenance. The metabolic burden is determined both by expression of plasmid-borne genes and the number of copies of plasmids within a cell (Diaz Ricci and Hernández, 2000; Friehs, 2004). The higher the copy number of the plasmid (hcn) is, the likely that the two daughter cells will contain the plasmid. However, hcn plasmids such as cloning vectors are most likely lost from populations at a high rate due to a large metabolic burden and lack of plasmid maintenance factors. Mechanisms to control vertical transmission of plasmids among bacterial hosts use different strategies, such as partitioning systems, random segregation and post-segregational killing.

Partitioning systems

An active partitioning system is common to low copy number plasmids and ensures that plasmids arising from pre-existing copies are segregated to daughter cells. Plasmids copies are organized around a centromere-like site and then separated into two daughter cells. *Par* systems consist of three components: a cis acting centromeric element, a motor protein and a DNA-binding protein that serves as an adaptor between the centromere and motor (Friedman and Austin, 1988). Adaptor binding of the centromere triggers polymerization of the motor which is together with filament formation essential for segregation. *Par* systems are auto-regulated by their own DNA-binding protein and independent of the cell cycle (Jensen *et al*., 1994; Jensen and Gerdes, 1999). Their classification is based upon the motor proteins they encode. Type I *par* systems feature Walker-A P-Loop ATPases whereas type II *par* systems are driven by actin-like ATPases (Hoischen *et al*., 2004; Ozyamak *et al*., 2013). Plasmids are pulled to the quarter-cell position prior to cell division in type I. Type II *par* systems bind and then separate plasmids to the cell poles by a pushing mechanism.

Random segregation

Hcn plasmids generally lack genes encoding active partition systems. However, they show considerable stability in the absence of positive selection which has been assigned to occasional generation of plasmid-free cells. This understanding, known as the random distribution model, assumes free distribution of plasmids throughout the cytoplasm before cell division and random segregation during cell division (Silva *et al*., 2012; Million-Weaver and Camps, 2014).

Post-segregational killing

Some plasmids ensure their transmission to the daughter cells through mechanisms that selectively kill plasmid-free daughter. For instance, plasmid-free daughter cells arising upon cell division are killed by cytoplasmic toxin once the immunity protein degrades cells (Hayes and Sauer, 2003; Stieber *et al*., 2008).

It was shown for *E. coli* that Soj belongs to the ParA ATPase protein family and can bind DNaA protein. Mutations introduced in Soj affected replication initiation indicating that Soj has an

effect on replication (Murray and Errington, 2008). However, the mechanism of its nonspecific binding to DNA remains unknown. A study in 2007 showed that Soj-DNA binding mutants are incapable of plasmid segregation suggesting that Soj in addition to having a dramatic effect on DNA binding is also involved in plasmid and chromosomal partitioning (Hester and Lutkenhaus, 2007).

Due to the limited data on the Soj protein, it was our goal to further investigate it. Work previously done in the lab by Prof. Witte showed the protein expression in the cell which starts 48 hours after inoculation of *N. magadii* L11 strain (Fig. 10).

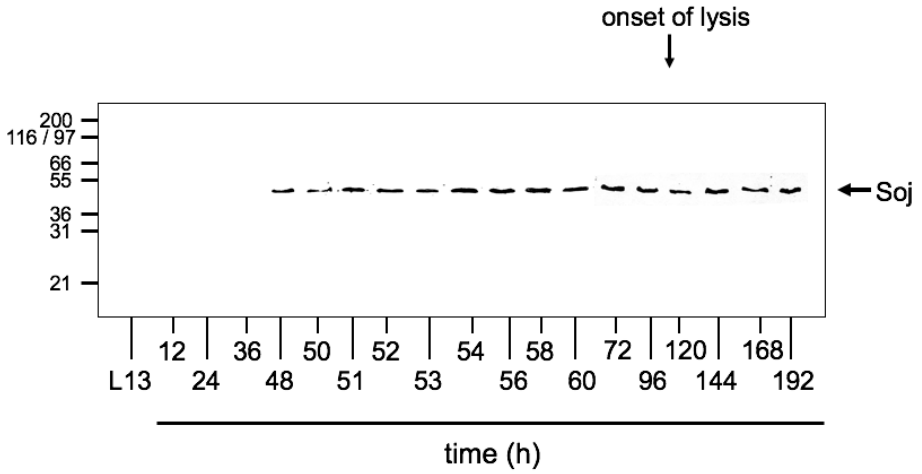

Figure 10. *Soj* expression in *N. magadii* L11. First detection of the protein Soj in *N. magadii* L11 is observable 48 h after inoculation and 3 days before onset of lysis (Witte A., unpublished data).

Our goal was to further investigate Soj by deleting its gene and to study its phenotype subsequently.

1.3.1.1.2. ORF49

As previously mentioned, the haloalkaliphilic virus ϕCh1 is a temperate virus that can switch between the lytic and lysogenic state. Regulating the switch between lytic and lysogenic state is of crucial importance. For this purpose, two open reading frames (ORFs) have been studied and identified as putative repressor encoding genes: ORF48 and ORF49. The gene product of ORF48

show sequence similarities to putative repressors. In contrast to ORF48, ORF49 was identified by analysis of the lysogenic strain carrying a mutant ϕCh1-1. For isolation of the mutant, cultures derived from single plaques were analyzed for differences in their lysis behaviors. It has been observed that the strain *N. magadii* L11-1 which harbors ϕCh1-1 lyses earlier than the strain L11. The lysis of the *N. magadii* L11-1 generally occurred on day 2 to 3 after incubation in comparison to the *N. magadii* L11 that lysed on day 3 to 4 (Fig. 11a). In addition, the plaques produced by the mutant strain were larger (Iro *et al*., 2007). To confirm further that the L11 strain contains the mutant, morphology, DNA methylation, RNA content and protein pattern were investigated and no difference was observable (Witte *et al*., 1997). However, Southern blot analysis showed in addition to the 1.9 kbp *Bgl*II-L fragment, a larger *Bgl*II fragment of 2.15kbp (L' fragment) that is present in ϕCh1-1 (Fig. 11b). Sequence analysis of this L' fragment revealed an insertion of 223 bp. This duplication is located upstream of ORF49 and created an additional ORF called ORF49' that codes for a putative 13.3 kDa protein. ORF49 and ORF49' slightly overlap and are most likely co-transcribed and co-translated. However, this additional insertion is rather instable since it tends to disappear after a few passages. The rate of lysis of the wild type was restored implying that this region is important for regulation of ϕCh1 in *N. magadii* (Iro *et al*., 2007).

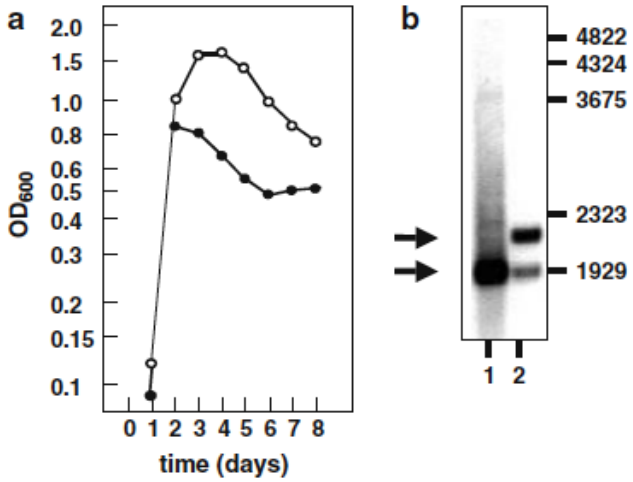

Figure 11. Earlier onset of lysis of *N. magadii* strain L11-1 in comparison to the wild type strain *N. magadii* L11 due to a short insertion within ϕCh1-1. a) Differences in lysis behavior of *N. magadii* L11 (open circle) and *N. magadii* L11-1 (black circle) studied by measuring the optical density at 600 nm of cells grown in rich medium for 8 days. **b)** Lane 1- ϕCh1 restricted with *Bgl*II; lane 2- ϕCh1-1 digested with *Bgl*II and analyzed by Southern blot (Iro *et al*., 2007).

For further analyses, the expression of ORF48 and ORF49 was monitored during the life cycle of *N. magadii* L11 by reverse transcriptase PCR (RT-PCR). ORF48 is constitutively expressed throughout the whole cycle of ϕCh1 (Fig. 12). It has been observed that most repressor genes of temperate viruses are only expressed during the lysogenic state. As ORF48 is constitutively expressed, an additional mechanism seems to be responsible for gene regulation in ϕCh1. Contrary to ORF48, ORF49 was not constitutively expressed. Its expression started 32h after inoculation of the *N. magadii* L11 strain. It has been observed that the intensity of the signal increases during the development of ϕCh1 indicating ORF49 gene product is expressed in the logarithmic and/or stationary growth phase (Fig. 12, lanes 7-13).

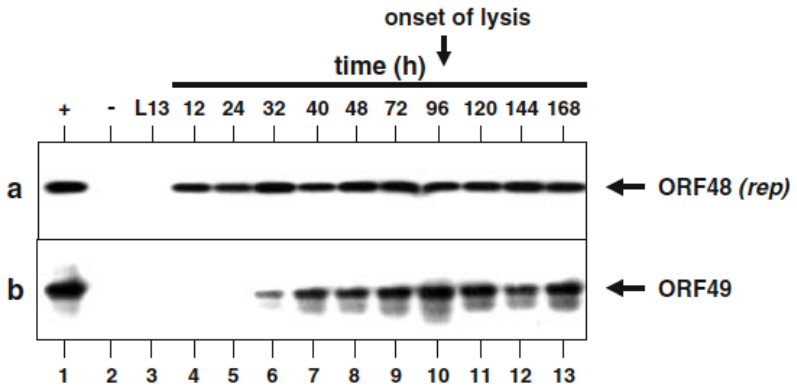

Figure 12. Expression of ORF48 (*rep*) and ORF49. Detection of ORF48 and ORF49 during the life cycle of *N. magadii* L11 using reverse transcriptase PCR. 0RF48 was constitutively expressed whereas the expression of ORF49 started 32h after inoculation (Iro *et al*., 2007).

Previous work in our lab demonstrated the effect of ORF49 on the infectivity of ϕCh1. ORF49 was transformed in *N. magadii* L13 and infected with ϕCh1. The resulted plaques were investigated and counted. As seen in figure 13, there is a reduction of plaque formation in the presence of ORF49 indicating that it is a putative gene repressor.

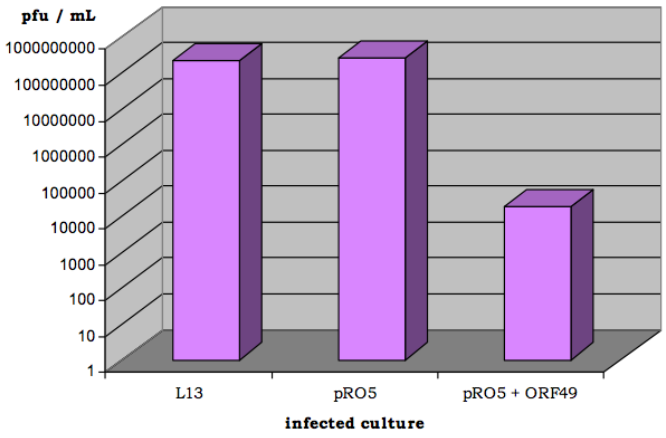

Figure 13. Repressor activity of ORF49. Phage titer analysis with plasmids pRo-4, pRo-5 and pRo-6 cloned in L13. Cloning of ORF49 within the plasmid pRo-5 reduces the plaque forming units indicating that ORF49 is repressor encoding gene (Reiter, 2010).

To further investigate ORF49, various versions with 3' truncated ends were created. Each fragment is shorter from the previous one by approximately 30-40 nucleotides. 70-80 nucleotides appear to be essential to maintain the repressor activity. The particularly crucial domains seem to be within 50 nucleotides.

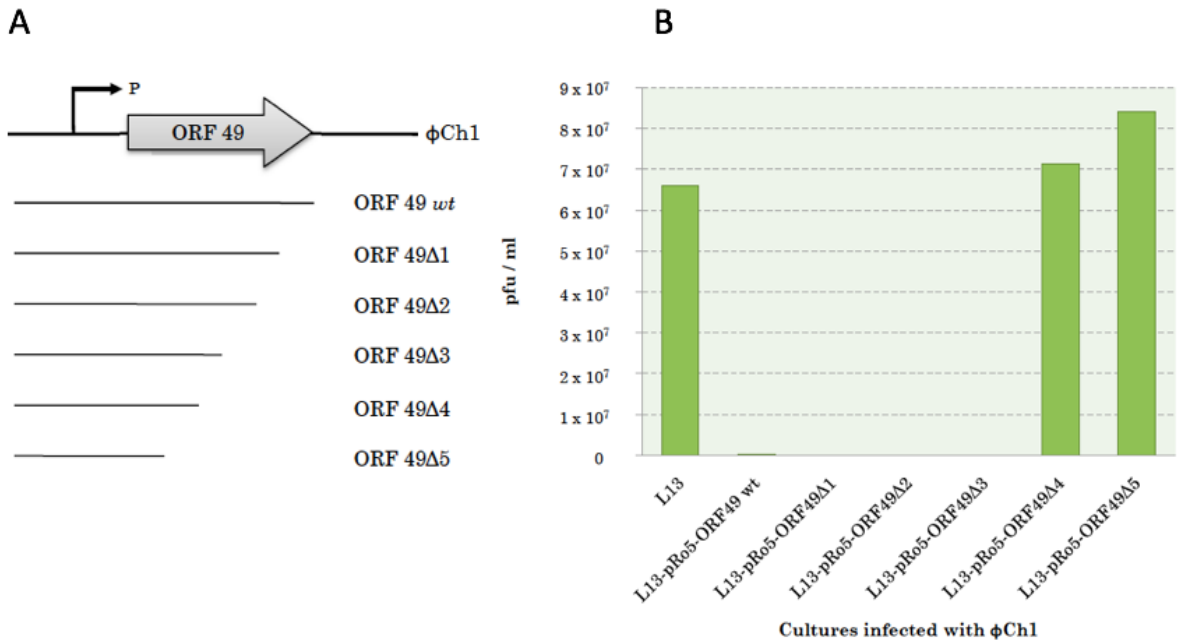

Figure 14. Repression activity of ORF49 C-terminal deletion mutants. A) Schematic representation of C-terminal deletion mutants. Each deletion mutant is shorter by 30-40 nucleotides. B) Phage titer analysis of C-terminal deletion mutants. The first three truncated versions show repressor activity. However, ORF49Δ4 and ORF49Δ5 appear to have lost their repressor activity (Reiter, 2010).

The N-terminus of ORF49 binds to DNA proven by EMSA (electrophoretic mobility shift assay) (Reiter, 2010).

In 2011, it was tried to delete ORF49. 379 base pairs were replaced with a novobiocin resistance cassette (NovR) which is on a suicide vector pKSII+ plasmid that cannot replicate in *N. magadii*. The disruption cassette was cloned in *N. magadii* strain L11 and by homologous recombination the exchange of the wild type with the novobiocin cassette should occur (Fig. 15).

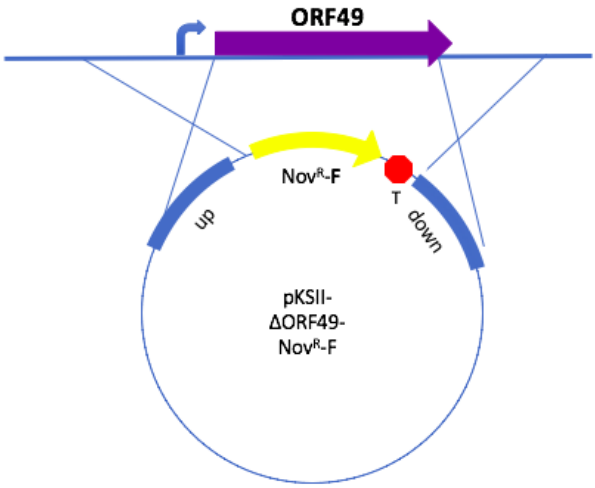

Figure 15. Schematic representation of deleted ORF49 with novobiocin in a forward direction. ORF49 was exchanged with the novobiocin resistance cassette in forward direction by homologous recombination.

However, Southern blot analysis showed that homogenization of ΔORF49 was not successful as shown in figure 16. Wild type ORF49 could still be detected in both putative ORF49 deleted strains (Fig. 16). Therefore, one of the goals of this thesis was to homogenize deleted version of ORF49 and compare its phenotype to the wild type *N. magadii* L11 strain.

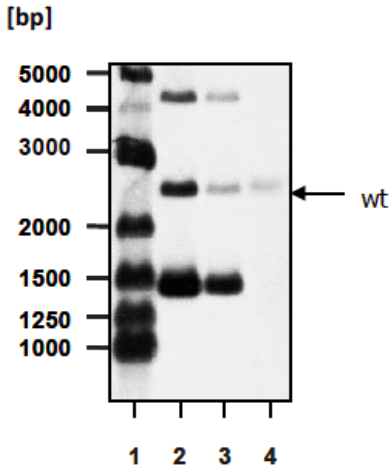

Figure 16. Southern blot analyses of *N. magadii* L11 and *N. magadii* L11-Δ49$_{1\text{-}2}$. Putative deleted strains of *N. magadii* L11 ORF49$_{1\text{-}2}$ (lane 3 and 4) show in addition the wild type band around 2663 bp (Svoboda, 2011).

2. Materials & Methods

2.1. Materials

2.1.1. Strains

2.1.1.1. *Escherichia coli*

Strain	Source	Genotype
XL1-Blue	Stratagene	*recA1*, *endA1*, *gyrA96*, *thi*, *hsdR17*(r_K^-, m_K^+), *supE44*, *relA1*, *lac*, [F', *proAB*+, *lacI*^{q}ZΔM15, Tn10(Tet^r)]

2.1.1.2. *Natrialba magadii*

Strain	Source	Genotype
L11	Witte *et al*., 1997	Wild type carrying provirus ϕCh1
L13	Witte *et al*., 1997	Cured strain lacking provirus ϕCh1

2.1.2. Media

2.1.2.1. Lysogeny broth (LB)

Reagents	**g/L**
Peptone	10
Yeast extract	5
NaCl	5
pH 7	
Agar for plates	15

2.1.2.2. NVM^{+}- Rich medium for *N. magadii*

Components	**g/L**
Casaminoacids	8.8
Yeast extract	11.7
Trisodium citrate	0.8
KCl	2.4
NaCl	235
pH 9-9.5	
Agar for plates	8
Agar for soft agar plates	4

NVM$^+$- Complementation of medium after autoclaving:

Components	Concentration	Total volume per liter
Na_2CO_3	0.57 M	65 ml
$MgSO_4$	1 M	1 ml
$FeSO_4$	20 mM	1 ml

2.1.3. Antibiotics and additives

Antibiotic	Stock concentration	Final concentration	Preparation
Ampicillin	20 mg/ml	100 μg/ml	Dissolved in ddH_20, sterile filtered, stored at 4°C
Tetracycline	10 mg/ml	10 μg/ml	Dissolved in half of ethanol and half ddH_20, stored at -20°C
Bacitracin	3 mg/ml	70 μg/ml	Dissolved in ddH_20, sterile filtered, stored at 4°C
Mevinolin	10 mg/ml	6 μg/ml	isolated from pulverized tablets, dissolved in 96 % ethanol, stored at -20°C
Novobiocin	7 mg/ml	3 μg/ml	Dissolved in ddH_20, sterile filtered, stored at -20°C

2.1.4. Primers

Primer Name	Sequence	Tm in °C
Nov-6	GGGATCGCAGAGGAGC	60,9
Nov-9	GATGTCGGTCATCGCGG	65,4
Nov-10	GAGGTCAAACACGACGGCG	68
Nov-11	GCATGTCGTGGCTGTTCG	65,6
Nov-12	GCCGGTGAGTACTTAACGC	61,1
Nov-13	GACGCCGAATGGGTAGAC	61,9
D49-2B	GACCGGATCCTTCCTGGGCCTCTTTGAA	62,1
49-XB	CAGCTCTAGAGGATCCTCATCCTGCGGTTTCG	54
49-1XB	CAGCTCTAGAGGATCCTCAGCCATTGGTCCGCGAGC	54
49-2XB	CAGCTCTAGAGGATCCTCAGCCCGGAAAGGACGACA	54
49-3XB	CAGCTCTAGAGGATCCTCAGCCTCTCACCGAGGCGC	54
49-4XB	CAGCTCTAGAGGATCCTCACAAGAACAGGAGAGTGTCCA	54
D49-3	GAC CAA GCT TAC GGG CCT GAC GCT TC	64
D49-41	GACCGGTACCCGCCTCGACCTGCTCCTG	64
44-Bam	CAGCGGATCCATGACGCTGTTCGTCG	58

ORF49-Nde	GAATCATATGAACACCCCCAATAGACA	60,4
ORF49-Bam	GTTAGGGATCCTCATCCTGCGGTTTCG	60,7
49-5-en	GCACTTGACGCGCCG	65,8
49-3-en	GCGTCACGGATCGATC	60,1
49-Kpn	CAGCGGTACCTTGCGTTCAGTTCCG	57,6
Soj-Up-Gi-1	CTCTAGAACTAGTGGATCCCCCGGGCTGCAGGAATTCGATCTGTTTGGCAACCTTCACTG	57
Soj-Up-Gi-2F	TCAGGAAATGACCTCGTTCCAGTCGACACACCCGGGGATCTCCCTGCTCCTCCTTTCTGG	59
Soj-Do-Gi-3F	TAACCAGACCGTTCAGCTGGATATTACGGCCTGCAGTAACGGAGGGATTCCATGGCTGAG	58
Soj-Do-Gi-4	CTGGGTACCGGGCCCCCCCTCGAGGTCGACGGTATCGATAGATCCAGAGGAGATCGCATC	56
Soj-Up-Gi-2R	TAACCAGACCGTTCAGCTGGATATTACGGCCTGCAGTAACTCCCTGCTCCTCCTTTCTGG	59
Soj-Do-Gi-3R	TCAGGAAATGACCTCGTTCCAGTCGACACACCCGGGGATCGGAGGGATTCCATGGCTGAG	58
Soj-Kpn	GATCGGTACCCGCGTTGCTCATCTGTTTG	64,4
Soj-3	CAGCAGCTGCAGCAGCAGTCAGCCATGGAATCCCT	60

ΔSoj-2	GAATACTAGTCTGGTTGGTAACTCCGATTC	59,8
ΔSoj-3	GAATAAGCTTGGAGGGATTCCATGGCTG	64,3
ΔSoj-4	GCCTGGTACCGATCCAGAGGAGATCGCATC	62,5
Δ53-1	GACCGAATTCGGATGCAAGCTGCTCGTGG	62,7
OR-1	CAGCAGAATTCAGGGTGACTGCCCTCG	56,2
SC-7	CAGCACAAGCTTGCAGAAGGCCTCCAAC	53
SC-21	CAGCACGGTACCATCGTGCGCCGATCG	59

2.1.5. Plasmids

Plasmid/Construct	Features	Source
pNB102	*bla*, ColE1 ori, *hmg* (Mev^R) pNB101 ori	Holmes *et al.*, 1991
Soj-pNB102	pNB102 containing ϕCh1 ORF46	This study
ORF49-Δ1	pNB102 containing deleted variants of C terminus ORF49	This study
ORF49-Δ2	pNB102 containing deleted variants of C terminus ORF49	This study
ORF49-C1	pNB102 containing deletion of middle part of ORF49	This study

ORF49-C2	pNB102 containing deletion of middle part of ORF49	This study
pKSII+	mcs, bla, ColE1 ori, lacZa	Stratagene
ΔORF49-NovR-F	pKSII+ with upstream and downstream region of ORF49 flanked by a novobiocin cassette in forward direction	This study
ΔORF49-NovR-R	pKSII+ with upstream and downstream region of ORF49 flanked by a novobiocin cassette in reverse direction	This study
ΔORF46(*soj*)-NovR-F	pKSII+ with upstream and downstream region of ORF46 flanked by a novobiocin cassette in forward direction	This study
ΔORF46(*soj*)-NovR-R	pKSII+ with upstream and downstream region of ORF46 flanked by a novobiocin cassette in reverse direction	This study

2.1.6. Enzymes

Enzyme[1]	Company	Product N°
Restriction enzymes	Thermo Scientific	/
DNA Polymerases		
Pfu DNA Polymerase	Promega	M7741
Phusion High Fidelity DNA Polymerase	Thermo Scientific	F530S
Go*Taq* DNA Polymerase/Mastermix	Promega	M3001/M7123
DNA modifying enzymes		
T4 DNA Ligase	Promega	M1801

2.1.7. Nucleotides

Name	Company	Product N°
dNTP Mix	Promega	U1511
Biotin-11-dUTP	GeneON	110

[1] All enzymes were used in combination with buffers recommended by company.

2.1.8. Ladders

DNA ladder	**Company**	**Size range in bp**
Lambda DNA *Bst*EII Digest	Thermo Scientific	702, 1264, 1371, 1929, 2323, 3675, 4324, 4822, 5686, 6369, 7242, 8454
GeneRuler 1kb DNA Ladder	Thermo Scientific	250 to 10000
GeneRuler 100 bp DNA Ladder	Thermo Scientific	100 to 3000
GeneRuler 50 bp DNA Ladder	Thermo Scientific	50 to 1000
Protein ladder		**Size range in kDa**
PageRuler™ Prestained Protein Ladder	Thermo Scientific	10, 15, 25, 35, 40, 55, 70, 100, 130, 170

2.1.9. Kits

Name	Company	Product N°
GeneJET Plasmid MiniPrep Kit	Thermo Scientific	K0503
Wizard®Plus SV Minipreps DNA Purification System	Promega	A1460
QIAquick® Gel Extraction Kit	QIAGEN	28706
GeneJET PCR Purficiation Kit	Thermo Scientific	K0701
Clarity™ Western ECL Substrate	BioRad	170-5061
Chemiluminescent Nucleic Acid Detection Module	BioRad	89880

2.1.10. Antibodies

Primary Antibody	Target	Dilution	Source
α-E (from rabbit)	Protein E of ϕCh1	1:2500	Klein *et al*., 2000
α-Soj (from rabbit)	Soj of ϕCh1	1:250	Hofbauer, 2015
Secondary Antibody			
ECL™ Anti-Rabbit IgG, HRP linked whole antibody from donkey	Rabbit Immunoglobulin G	1:5000	GE Healthcare, N°-NA934

2.1.11. Solutions and buffers

2.1.11.1. Competent cells

2.1.11.1.1. *E. coli*

MOPS I

MOPS	100 mM
KCl	10 mM
RbCl	10 mM
pH 7[2]	

MOPS II

MOPS	100 mM
KCl	10 mM
RbCl	10 mM
pH 6.2	

MOPS IIa

MOPS	100 mM
KCl	10 mM
RbCl	10 mM
Glycerol 15 %	
pH 6.2	

2.1.11.1.2. *N. magadii*

Buffered high salt spheroplasting solution

NaCl	2 M
KCl	27 mM
Tris/HCl	pH 8
15 % filtered sucrose (after autoclaving)	

Buffered high salt spheroplasting solution with glycerol

NaCl	2 M
KCl	27 mM
Tris/HCl	pH 9.5
15 % glycerol	
15 % filtered sucrose (after autoclaving)	

[2] pH for all MOPS solutions was adjusted with KOH.

Unbuffered high salt spheroplasting solution

NaCl	2 M
KCl	27 mM

15 % filtered sucrose (after autoclaving)

60 % PEG600

PEG 600	60 %
UHSSS[3]	40 %

2.1.11.2. Isolation of virus ϕCh1 particles

High-salt alkaline solution

Tris/HCl pH 9.5	50 mM
NaCl	4 M

1.1 CsCl solution

Tris/HCl pH 8.5-9	50 mM
NaCl	2 M
CsCl	0.6 M

1.3 CsCl solution

NaCl	2 M
Tris/HCl pH 8.5-9	50 mM
CsCl	3.7 M

1.5 CsCl solution

NaCl	2 M
Tris/HCl pH 8.5-9	50 mM
CsCl	4 M

2.1.11.3. DNA gel electrophoresis

50x TAE

Tris/HCl pH 8.2	2 M
Acetic acid	1 M
EDTA	0.1 M

0.8 % agarose

agarose melted in 1x TAE

5x DNA Loading Dye

Tris/HCl pH 8.2	50 mM
SDS	0.1 %
Bromphenol blue	0.05 %
Xylene cyanol	0.05 %

25 % filtered sucrose (after autoclaving)

[3] UHSSS- unbuffered high salt spheroplasting solution

2.1.11.4. Polyacrylamide gel

2.1.11.4.1. Protein extracts

2x Laemmli buffer

SDS	2 %
β-mercaptoethanol	5 %
Glycerol	10 %
Bromphenol blue	0.01 %
Tris/HCl pH 6.8	60 mM

5 mM sodium phosphate buffer pH 6.8

NaH_2PO_4	0.2 M
Na_2HPO_4	0.2 M

2.1.11.4.2. SDS-PAGE

6 % Polyacrylamid solution

30 % PAA	40 ml
1x TBE	160 ml

1x TBE

Tris	108 g
Boric acid	60 g
0.5 M EDTA pH 8	40 ml

30 % Acrylamide solution

Acrylamide	29 %
N, N'-methylenebisacrylamide	1 %

Separating gel buffer

Tris/HCl	pH 8.8
SDS	0.4 %
ddH_2O ad 250 ml	

Stacking gel buffer

Tris/HCl	pH 6.8
SDS	0.4 %
ddH_2O ad 250 ml	

10x SDS running buffer

Tris	0.25 M
Glycin	1.92 M
SDS	1 %

Coomassie staining solution

Methanol	25 %
Acetic acid	10 %

Coomassie destaining solution

10 % acetic acid in ddH_2O

Coomassie Briliant Blue R-250	0.15 %

2.1.11.5. Western Blot

10x TBS

Tris/HCl pH 8	0.25 M
NaCl	1.37 M
KCl	27 mM

Transblot buffer

Tris	48 mM
Glycine	39mM
SDS	0.037 %
Methanol	20 %

Blocking solution

Milk powder	5 % in 1x TBS

Primary antibody

BSA	0.3 %
NaN_3	0.02 %

Respectively dilutes serum
Spatula of L13 acetone powder

Secondary antibody

Commercialized 2nd antibody diluted in ratio 1:5000 in 1x TBS

2.1.11.6. Southern Blot

20x SSC

NaCl	3 M
Na-citrate	0.3 M
pH	7.2

50x Denhardt's solution

BSA	1 g
Polyvinylpyrolidone	1 g
Ficoll 400	1 g

ddH_2O ad 100 ml

Blocking solution

NaCl	7.3 g
Na_2HPO_4	2.41 g
NaH_2PO_4	0.96 g
SDS	49.89 g
pH	7.2

Hybridization buffer

20x SSC	25 ml
Denhardt's solution	10 ml
10 % BSA	5 ml
1 M Na_2HPO_4	5 ml
20 % SDS	500 µl
0.5 M EDTA	200 µl
ddH_2O ad 50 ml	

10x Wash solution II

Tris	12.1 g
NaCl	5.85 g
$MgCl_2$	2.03 g
pH	9.5

2.2. METHODS

2.2.1. DNA Methods

2.2.1.1. Polymerase chain reaction (PCR)

2.2.1.1.1. Templates for PCR

Depending on experiment, different templates were created:

1) Purified ϕCh1 DNA (1:30 diluted)
2) Templates from *E. coli* or *N. magadii* (undiluted)

   Templates were created by centrifuging 30 µl of culture for 3 minutes at 13 krpm and resuspending the pellet in 100 µl ddH_20.

Polymerase chain reaction was used to amplify DNA. Here, two different PCRs were carried out using two different polymerases: preparative PCR using *Pfu* polymerase, which has a superior thermostability and proofreading activity as well as the 3'-5' exonuclease activity. Therefore, *Pfu* polymerase is more accurate in comparison to the *Taq* Polymerase, which was used for analytical PCR to search for positive transformants after cloning. The elongation time depends on the polymerase. *Pfu* polymerase inserts 500 bp per minute whereas the *Taq* polymerase 1000 bp per minute.

Preparative PCR	**Volume in µl**	**Analytical PCR**	**Volume in µl**
2mM dNTPs	10	2x *GoTaq* Green MasterMix	12.5
10x *Pfu* 10x reaction buffer	10	Forward primer (0.1 ug/µl)	1.5
Forward primer (0.05 µg/µl)	5	Reverse primer (0.1ug/µl)	1.5

Reverse primer (0.05 μg/μl)	5	Template	1
Template DNA	1	ddH_20	8.5
ddH_20	67		
Pfu Polymerase (2-3U/μl)	2		

2.2.1.1.2. PCR Program

Step	**Temperature (°C)**	**Duration (min)**	**Number of cycles**
Initial denaturation	95	4	1
Denaturation	95	1	35 (preparative) 20 and 50 (for analytical)
Annealing	Tm*	1	
Elongation	72	Time*	
Final elongation	72	2x time	1

Tm*- depends on primers' composition.
Time*-depends on PCR product length as well as on the polymerase type.

2.2.1.1.3. Quality control of PCR product

The quality of PCR product was controlled on 0.8 % agarose gel. For preparative PCR products, 5 μl of 5x DNA loading dye were mixed together with the sample and applied on gel whereas analytical PCR probes could be directly loaded on the gel.

2.2.1.2. Agarose gel electrophoresis

Separation of DNA fragments by size was performed by electrophoresis in agarose, which was previously dissolved in 1x TAE buffer (end conc.: 0.8 % or 1.2 %, depending on the size of

fragments). Prior loading, the samples were mixed with DNA loading dye. The power applied was 100 V for small gel and 170 V for big gel. Afterwards, the bands were stained in an ethidium bromide bath (800 μl/800 ml ddH_20), rinsed for a short period of time in ddH_20 and visualized by UV light.

2.2.1.3. 6 % Polyacrylamide (PAA) gel electrophoresis

Polyacrylamid gel electrophoresis, particularly 6 % PAA was used for separation of DNA fragments smaller than 700 bp. whereas SDS-PAGE was used to separate proteins. The gel was prepared in BioRad Mini- Protean R apparatus. The samples were prepared in the same way as for agarose gel electrophoresis. The gels were run by applying power of 40 V (20 mA) until the dye used in preparing DNA samples reached the end of the glass plate. Afterwards, the gels were left on one glass plate and as such stained in ethidium bromide bath, rinsed in ddH_20 and visualized with UV light.

2.2.1.4. DNA purification

2.2.1.4.1. PCR product purification

PCR products were purified using GeneJET PCR purification Kit (Thermo Scientific) to eliminate all undesirable products. Purified PCR product was eluted in 50-100 μl ddH_20, depending on the desired final concentration.

2.2.1.4.2. DNA gel elution and purification

Gel elution was essential in case errors occurred during PCR amplification. The fragment was restricted and separated on 0.8 % agarose gel. Desired bands were visualized using 70% UV light intensity and purified according to the protocol from QIAquick® Gel Extraction Kit. The purified DNA fragment was eluted in 50-100 μl ddH_20.

2.2.1.5. DNA concentration measurement

DNA concentrations were estimated using spectrophotometer NanoDrop™ ND-2000c from Thermo Scientific.

2.2.1.6. DNA Restriction

Restriction of DNA fragments was performed using restriction enzymes from Thermo Scientific. Digestion was achieved at 37°C either for 3 h or overnight. The success of restriction was analyzed on agarose gel electrophoresis together with unrestricted plasmid. According to the size of band, the plasmid was diluted in ratio of 1:10 or 1:20.

Protocol:

DNA	30 µl
Restriction enzyme	2 µl
Buffer	5 µl
ddH_2O	11 µl

2.2.1.7. DNA Ligation

For further cloning, DNA sequence of interest and plasmid were ligated using T4 Ligase and 10x T4 Ligase buffer from Promega. The ligation batch was incubated either for 3 h at room temperature or overnight at 4°C.

Protocol:

DNA fragment	11.5 µl
Plasmid	1 µl
T4 ligase buffer	1.5 µl
T4 ligase	1 µl

The total volume of ligation reaction (15 µl) was used for transformation into *E. coli.*

2.2.2. Transformation into *E. coli*

2.2.2.1. Competent cells

Obtaining *E. coli* competent cells was achieved by inoculating XL1-Blue strain in 200ml of LB with respective antibiotic to on OD_{600} of 0.1. When the culture reached OD_{600} of 0.6, the cells

were centrifuged for 10 minutes at 10 krpm at 4°C. The pellet was resuspended in 80 ml MOPS I and incubated for 10 minutes on ice. After resuspension, the centrifugation was performed again under same conditions. Next, the pellet was resuspended in 80ml MOPS II and incubated for 30 minutes on ice. Afterwards, final centrifugation step was performed at 10 krpm for 10 minutes at 4°C and resuspended in 4 ml MOPS IIa. Competent cells were aliquoted in Eppendorf tubes (100 µl each) and stored at -80°C.

2.2.2.2. Transformation

The competent *E. coli* cells were thawed on ice for 10 minutes. The ligation mix (15 µl) was added to the competent cells. The reaction mix was incubated on ice for 30 minutes followed by a heat shock at 42°C for 2 minutes. Afterwards, ligation mix was incubated shortly on ice and 300 µl LB were added to the mix Regeneration of cells occurred at 37°C for 30 minutes without shaking. 100 µl of transformation batch was plated on LB/agar plates with the appropriate antibiotic and incubated overnight at 37°C.

2.2.2.3. Quick plasmid preparation for screening of positive transformants

The colonies visible from the plates were inoculated in test tube containing 5 ml LB and ampicillin. The tubes were incubated overnight at 37°C. Next day, 300 µl of the culture were centrifuged at maximum speed for 3 minutes at RT. The pellets were resuspended in 30 µl of 5x DNA loading dye and vortexed for 20 seconds. Next, 14 µl of phenol-chloroform (1:1) was added and subsequently vortexed. Afterwards, the samples were centrifuged at maximum speed for 5 minutes at RT and 12 µl of the supernatant that contains chromosomal DNA, plasmid DNA and RNA were loaded on 0.8 % agarose gel.

2.2.2.4. Confirmation and storage of positive transformants

The obtained plasmids were tested for an inserted DNA performing analytical PCR using Taq polymerase. 1 µl of the culture was used as template. After verifying the positive clone, 100-200 µl of the positive transformant was inoculated into 20 ml LB with ampicillin and tetracycline. Afterwards 1 ml of the positive clone was mixed with 800 µl of 50 % glycerol and stored at -80°C.

2.2.3. Transformation into *N. magadii*

2.2.3.1. Competent cells

N. magadii competent cells had to be grown in NVM^+ with Bacitracin (final conc. 70 μg/ml) in buffle flasks to an OD_{600} of 0.5 to 0.6. The cells were harvested at 6 krpm for 15 minutes at RT. The cell pellet was resuspended in half of the volume of high salt buffered spheroplast solution with glycerol and Proteinase K was added (final conc. 0.1 %). Next, the cells were incubated at 42°C for app. 48 hours until they were transformed into spheroplasts.

2.2.3.2. Transformation

Frozen cells (1.5 ml) were thawed at room temperature and centrifuged for 3 minutes at 10 krpm. The pellet was resuspended in 150 μl of high salt spheroplast solution without glycerol and 15 μl of 0.5M EDTA was added. After 10 minutes of incubation at RT, maximum 10 μl of DNA (final conc. 3-5 μg or 20-40 μg for deletion mutants) were added and incubated at RT for 5 minutes. Next, 150 μl of PEG 600 (previously mixed with high salt unbuffered solution to the final concentration of 60 %) were added and subsequently incubated at RT for 30 minutes. 1 ml of NVM^+ was added and centrifuged for 5 minutes at 10 krpm. Cells were resuspended in 1 ml NVM^+. Washing was repeated twice and the cells were incubated at 37°C for one to two days. The cells that looked like rods were ready to be plated on rich medium agar plates with relevant antibiotics and incubated at 42°C for two to three weeks.

2.2.3.3. Screening of positive transformants

After a successful transformation, the colonies were each inoculated into 500 μl of NVM^+ in Eppendorf tube and incubated at 37°C for a couple of days until growth was visible. Meanwhile, the cultures were shortly aired to improve their growth. Afterwards, cell templates (see 2.2.1.1.1) were prepared and the cultures were tested by analytical PCR.

2.2.4. Homogenization of *N. magadii* L11 deletion mutants

N. magadii has around 50 copies of its genome. Therefore, it was a prerequisite to perform homogenization of a deleted mutant. Thus, every copy of the viral ORF should be deleted. In order to yield homozygous deletion mutant, mutant virus particles had to be isolated and then infected with *N. magadii* L13.

Lysis of the culture containing mutant lysed, meaning that the virus particles were released. At that time, the culture was centrifuged at 12 krpm for 20 minutes at room temperature. 20 µl of chloroform was added to the supernatant to avoid growth of the remaining cells. A *N. magadii* L13 culture was grown to an OD_{600} of 0.55. 100, 200, 300, 400, 500 µl of the lysate were added to *N. magadii* L13 and incubated for 1.5 h at 37°C. Cells were centrifuged for 5 minutes at 10 krpm at RT and resuspended in 500 µl NVM^+. 200 µl were plated out on the rich medium agar plates containing novobiocin. The plates were incubated at 42°C until colonies were visible. These colonies were tested by PCR for homozygous deletion mutants.

2.2.5. ϕCh1 methods

2.2.5.1. Isolation of virus particles

2 x 2.5 L of the strain were inoculated to an OD_{600} of 0.1. and incubated at 37°C. The optical density was measured every day until the culture lysed. Next, the culture was centrifuged at room temperature for 20 minutes at 6000 x g. The virus particles that remained in the supernatant were coated with PEG 6000 (final concentration 10 %) and stirred overnight. Afterwards, they were collected by another centrifugation step for 20 minutes at 6 000 x g at RT. The pellet was resuspended in high salt alkaline solution (see 2.1.11.2). For further purification, a discontinuous CsCl gradient was performed. For that reason, the ultra-centrifuge tubes were filled with 3.5 ml of 1.5 CsCl, 4 ml of 1.3 CsCl, 5 ml of virus suspension and balanced out with 1.1 CsCl solution. The tubes were centrifuged for 20 hours at 30 000 rpm at RT. A blue band was visible which represents desired virus particles. The next step was purification of this

blue band by performing a continuous gradient in which only 1.3 CsCl solution was used and centrifuged for 20 hours at 30 000 rpm at RT. Afterwards the virus particles were dialyzed against high salt alkaline solution (4 M NaCl, 50 mM Tris/HCl, pH 9.5) to remove all Cs^+ ions first for one hour and then the buffer was changed and dialysis was took place overnight.

2.2.5.2. Isolation of viral DNA

3x 100 µl of viral suspension were mixed with 400 µl of ddH_20 and 400 µl of Phenol/Chloroform (1:1) was added and vortexed for 20 seconds. Next, this suspension was centrifuged for 2 minutes at 13 krpm at RT. The supernatant was transferred into a new Eppendorf tube and the Phenol/Chloroform extractions were repeated until no white interphase was visible. Next, the supernatant which contained DNA was mixed with 800 µl of isopropanol and centrifuged for 30 minutes at 4°C at 13 krpm. Subsequently, the pellet was dried at 65°C with the lid opened and dissolved in 10 µl ddH_2O.

2.2.5.3. Plaque assay

In order to determine the viral titer per ml, a plaque assay had to be performed. Dilutions (10^{-2} to 10^{-10}) of isolated virus were prepared to infect *N. magadii* L13 and different constructs cloned into *N. magadii* L13. Therefore, 100 µl of the viral dilution were mixed with 300 µl of *N. magadii* L13 in 5 ml rich medium soft agar that was previously warmed at 55°C. Next, the soft agar was poured on rich medium agar plates. The plates were incubated at 37°C and after a couple of days, the plaques were counted in order to determine the virus titer (plaque-forming units/pfu per ml).

2.2.6. Southern Blot

Southern Blotting detects a specific DNA sequence in DNA samples. It includes three steps: separation of DNA fragments by gel electrophoresis, transfer of separated DNA fragments to a nylon membrane (GE Healthcare Amersham Hybond™-N) and subsequent fragment detection via probe hybridization.

- Probe synthesis

The probes were synthesized by PCR using a *GoTaq* Green Mastermix enriched with biotinylated dUTPs that were previously diluted with TE buffer in ratio 1:5. The probes were eluted from 0.8 % agarose gel using Wizard®SV Gel and PCR Clean-Up System. Afterwards the probes were eluted in 50 µl of ddH_2O.

PCR protocol for probe synthesis:

Components	**Final volume in µl**
GoTaq Green Mastermix	50
Primer 1	10
Primer 2	10
Template	1
Biotinylated dUTPs	2.5
ddH_2O	26.5
Total Volume	100

- DNA restriction

After isolation of viral DNA, it was restricted overnight with *Bam*HI restriction enzyme. 3 µl of restricted viral DNA were loaded on 0.8 % agarose together with the wt ϕCh1. After successful restriction, DNA could be blotted.

- Blotting of DNA to a nylon membrane

Before blotting, DNA had to be denatured in 0.4 M NaOH/ 0.6 M NaCl for 30 minutes and neutralized in 1.5 M NaCl/ 0.5 M Tris/HCl pH 7.5 for 30 minutes. Meanwhile the capillary blot was built according to the following procedure: Whatman paper was put in agarose gel electrophoresis chamber filled with 10x SSC buffer; three pieces of Whatman paper having a size of gel were put in the middle and on top of them was agarose gel followed by the nylon membrane that was previously equilibrated in 10x SSC. On top were put another three Whatman papers. To construct a tighter blot ensuring the transfer of DNA fragments to the nylon membrane, a stash of paper towels compressed by a lid of electrophoresis chamber was used. Blotting occurred overnight. Subsequently, the membrane was incubated in 0.4 M NaOH and 0.2 M Tris/HCl pH 7.5 for 1 minute. Next, the blotted DNA fragments on the nylon membrane were fixed via UV-crosslinking.

- Membrane blocking and hybridization

To prevent unspecific probe binding, the membrane was previously blocked at 65°C for 3 hours in 12 ml of hybridization buffer and 120 μl of salmon sperm DNA (10 mg/ml) in a rotary incubator. The probes were denatured for 10 minutes at 95°C and added to the hybridization tube in which the membrane was. The hybridization took place overnight in a rotary incubator at 65°C.

- Blot development

After hybridization, the membrane was washed twice in 2x SSC/ 0.1% SDS and for 5 minutes at RT and additionally in 0.1x SSC/ 0.1% SDS twice for 15 minutes in 65°C rotary incubator. The blot was developed using BioRad Clarity™ Western ECL Substrate Kit.

2.2.7. Protein methods

2.2.7.1. Protein crude extracts preparation

For characterization of proteins by Western blot, crude extracts had to be prepared. Thus, 1.5 ml of culture was centrifuged for 3 minutes at 13 krpm. The supernatant was saved for virus titer analysis whereas the pellet was resuspended in 5 x mM sodium phosphate buffer and 2x Laemmli buffer. Volume of buffers was determined according to the OD_{600} nm: OD_{600} x 75. *N. magadii* extracts were incubated at 37°C overnight.

2.2.7.2. SDS-PAGE

Proteins were separated by SDS-PAGE (sodium dodecyl sulfate polyacrylamide gel electrophoresis) according to their molecular weight. Anionic detergent, SDS, disrupts the tertiary structure of the proteins and coats them with the negative charge.

The gel matrix used for SDS-PAGE is polyacrylamide which is chemically inert, and consists of two parts, a separation and stacking gel. The gels were prepared using BioRad-Mini-PROTEAN apparatus. The separation gel (12 %) was prepared first. Isopropanol was immediately added on the top of the running gel to avoid bubbles. After polymerization, the isopropanol was removed and the stacking gel (4 %) was poured on top. A 10-well comb was gently placed between the two glass plates. After polymerization, the combs were removed and 1x SDS running buffer was poured between two gels and in the chamber. Finally, the samples together with protein ladder could be loaded. *N. magadii* crude extracts were separated at 40 V due to high salt concentration of the samples.

2.2.7.3. Coomassie staining

Determination of protein concentration after their separation using SDS-PAGE can be achieved by staining them with Coomassie Brilliant Blue dye. The dye binds to proteins through ionic interactions between sulfonic acid groups and positive protein amine groups as well as through Van der Waals attractions. The gel was stained in Coomassie Blue solution for 30 minutes while covered and shaking. Destaining followed in order to visualize the bands. This was achieved by

incubating the gel in destaining solution. After sufficient destaining, the protein bands were visible and therefore their protein concentration for performing Western Blot could be determined.

2.2.7.4. Western Blot

Western Blotting is often used method to separate and identify specific proteins in a sample. The technique includes three tasks: 1) separation by size using SDS-PAGE, 2) transfer to a nitrocellulose membrane, 3) marking the target protein using a proper primary antibody that recognizes the separated proteins and a secondary antibody that is coupled to a reporter enzyme horseradish peroxidase (HRP), which cleaves a chemiluminescent agent, thus producing luminescence in proportion to the amount of protein.

- Transfer to a membrane

  The transfer was done using an electric field, and thus causing proteins to move out of the gel and onto the membrane. First, three filter papers (9 x 6 cm) were pre-wet in transfer buffer one by one and put on the blotting device (Bio Rad Trans-Blot^{R} Turbo^{TM} Transfer System). Then the nitrocellulose membrane (GE Healthcare Amersham^{TM} Protran^{TM} 0.2 μm NC) was also pre-wet in transfer buffer and put on top of the filter papers. The gel was gently transferred into the blotting buffer and set on the top of the membrane. The other three filter papers were pre-wet in blotting buffer as well and put on the top of the gel to protect it. Next, we used a rolling device to eliminate all air bubbles. Finally, a voltage of 25 mA per one or two mini gels were applied. So, the negatively charged proteins migrate from the gel to the membrane in a semidry blot. After blotting, the overall effectiveness of proteins' transfer could be checked by staining the membrane with Ponceau S dye for a couple of minutes to visualize the bands. After visualization, the membrane was destained with tap water.

- Blocking

To prevent nonspecific binding of antibodies to the membrane, the membrane was incubated in skimmed milk solution (5 % milk powder dissolved in 1x TBS) overnight at 4°C.

- Use of antibodies

After blocking, 10-15 ml of the primary antibody could be applied for one hour while gently shaking. α-Soj antibody was diluted to 1:250 whereas α-E 1:2000 or 1:2500 dilution was diluted to a final concentration of 0.3 % BSA and 0.02 % NaN3. In addition, one spatula of acetone powder from *N. magadii* L13 was added to saturate the antibodies. The membrane was washed three times 10 minutes with 1x TBS and incubated with the secondary antibody that was always fresh prepared (1:5000 in 1x TBS) for one hour as well. Subsequently, it was washed again three times with 1x TBS. The secondary antibody recognizes and binds to the conserved IgG domain of the primary antibody and is coupled to horse radish peroxidase (HRP).

- Detection

Detection was performed using Bio-Rad Clarity™ Western ECL Substrate Kit. The membrane was incubated for 5 minutes and the blot could be detected using ImageLab program. Exposure was performed from 10 up to 60 or 120 seconds. Detection of the protein of interest is based on a chemiluminescent reaction. Horse radish peroxidase (HRP), which is linked to the secondary antibody, catalyzes the oxidation of the chemiluminescent substrate luminol. The visible light is generated by decaying of the oxidized luminol to its ground state. After washing off the secondary antibody with 1x TBS, 1 ml of HRP Substrate Luminol Reagent and 1 ml of HRP Substrate Peroxide Solution were mixed per one membrane (Immobilon Reagent) and put on the membrane. A sensitive sheet of the photographic film is placed against the membrane and exposure to the X-ray film for a proper duration mentioned above allowing the blot to be developed.

2.2.8. Cloning strategies

2.2.8.1. ORF49 deletion mutants

The upstream region of ORF49 was amplified via PCR using ϕCh1 DNA template and primers Δ49-1-X and Δ49-2-B that yielded a length of 1020 bp. The fragments were restricted with *Xba*I/*Bam*HI and ligated into pKSII+ previously restricted with the same restriction enzymes. The

constructed plasmid was named pKSII_fragment1. Downstream region was cloned using primers Δ49-3 and Δ49-41 with a total length of 703 bp. The fragment was restricted with *KpnI/Hind*III and ligated into pKSII_fragment1 that was digested with the same restriction enzymes as well. Positive clones were named pKSII_fragment1_fragment2. Novobiocin cassette (2453 bp) was isolated from pUC19-NovR "forward" and pUC19-NovR "reverse" with the restriction enzymes *Sma*I and *Pst*I. Novobiocin cassettes were cloned into vectors previously described and named pKSII_d49_novF_d49 and pKSII_d49_novR_d49. These plasmids were transformed into *N. magadii* L11.

2.2.8.2. ORF49Δ1- pNB102

The fragment was amplified from ϕCh1 using primers 49-Kpn and 49-1XB. After purifying the fragment, it was restricted with *Kpn*I and *Xba*I. The plasmid pNB102 was linearized with the same restriction enzymes. After successful restrictions, the fragment and plasmid were ligated.

2.2.8.3. ORF49Δ2- pNB102

Primers 49-Kpn and 49-2XB together with ϕCh1 DNA were used for creation of ORF49Δ2 fragment. Next, the fragment and plasmid pNB102 were linearized with *Kpn*I and *Xba*I restriction enzymes and ligated.

2.2.8.4. ORF49-C1- pNB102

This fragment was amplified from pUC-promoter-cterm1 with primers 49-Kpn and 49-XB. Insert and vector pNB102 were restricted with *Kpn*I and *Xba*I. After successful restriction, ORF49-C1 and pNB102 were ligated.

2.2.8.5. ORF49-C2- pNB102

ORF49-C2 was amplified by PCR with primers 49-Kpn and 49-XB. However, in comparison to ORF49-C1, the template pUC-promoter-C2 was used. Fragment and vector pNB102 were digested with *Kpn*I and *Xba*I and ligated.

2.2.8.6. ORF46 (*soj*) deletion mutants

Construction of deletion variants of ORF46 with novobiocin resistance cassette in forward and reverse direction was performed with the Gibson assembly method. Gibson assembly reaction allows joining of multiple DNA fragments in a single reaction. It requires enzyme activity of exonuclease which chews back DNA from 5' end, DNA polymerase and DNA ligase. Deletion of *soj* with the novobiocin resistance cassette in forward and reverse orientation (ΔsORF46(*soj*)-NovR-F and ΔORF46(*soj*)-NovR-R) was achieved by PCR with ϕCh1 template. Upstream region of ΔORF46(*soj*)-NovR-F was amplified with primers Soj-Up-Gi-1 and Soj-Up-Gi-2F whereas for amplification of upstream region of ΔORF46(*soj*)-NovR-R primers Soj-Up-Gi-1 and Soj-Up-Gi-2R were used. Downstream region of ORF46 deletion mutant with novobiocin in forward direction was created with primers Soj-Up-Do-3F and Soj-Up-Gi-4. Downstream region of ΔORF46(*soj*)-NovR-R was amplified with Soj-Up-Do-3R and Soj-Up-Gi-4. Plasmid pKSII+ was restricted with *Eco*RV and *Hind*III and novobiocin resistance (2453 bp) was isolated from pUC19-NovR "forward" and purified. Gibson assembly reaction was performed in one step by mixing PCR products, pKSII and novobiocin cassette together, incubating it 1 hour at 50°C and plating on ampicillin/tetracycline LB plates. After positive screening of transformants into XL1-Blue, clones were transformed into *N. magadii* L11.

2.2.8.7. *soj*-pNB102

ORF46 was amplified via PCR from ϕCh1 DNA using primers Soj-Kpn and Soj-Xba. The purified PCR fragment was restricted with *Kpn*I and *Xba*I and ligated into pNB102 that was previously digested with the same restriction enzymes.

3. Results & Discussion

3.1. ORF46 (*soj*)

3.1.1. Aim

ϕCh1 ORF46 codes for Soj protein that is characterized as a putative plasmid partitioning protein. Very few studies investigated the potential function of Soj. In addition, one study in 2015 demonstrated that Soj has an influence on the plasmid pNB102 stability. In the presence of Soj, the plasmid pNB102 was lost in *N. magadii* L13 which further confirms that Soj might be indeed a plasmid partitioning protein causing the loss of the plasmid (Hofbauer, 2015). Therefore, our aim was to delete ORF46 that encodes the protein Soj in *N. magadii* L11 in order to further investigate the function of Soj.

3.1.2. Construction of pKSII-ΔORF46(*soj*)-NovR-F and pKSII-ΔORF46(*soj*)-NovR-R

Plasmid pBlueScript II KS + (pKSII+) was used for the construction of *N. magadii* L11-pKSII-ΔORF46(*soj*)-NovR-F and *N. magadii* L11-pKSII-ΔORF46(*soj*)-NovR-R since it lacks the origin of replication for *N. magadii*. Upstream and downstream regions of ORF46 were separated by the novobiocin resistance cassette in forward and reverse direction enabling the growth of only those cells in which exchange between ORF46 and novobiocin resistance cassette occurred (see 2.2.8.6). Schematic overview of construction of *N. magadii* L11-pKSII-ΔORF46(*soj*)-NovR-F and *N. magadii* L11-pKSII-ΔORF46(*soj*)-NovR-R is given in figure 17.

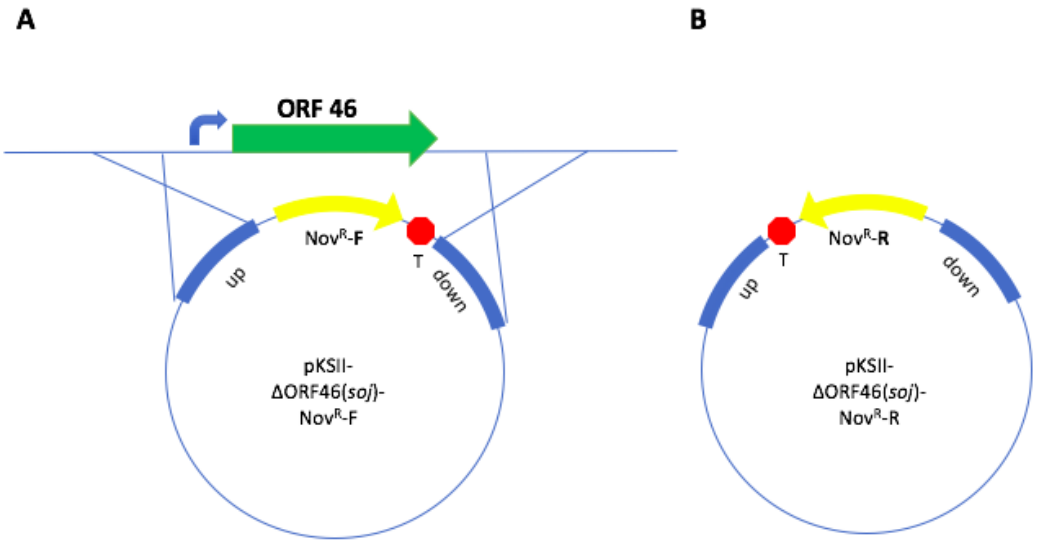

Figure 17. Schematic overview of construction of ORF46 (*soj*) deletion mutants. Blue arrow indicates ORF46 promoter. Two orientations of novobiocin resistance cassette (**A)** forward and **B)** reverse) are represented as yellow arrows. Flanking regions marked blue are essential for homologous recombination. Terminator sequence which ensures the end of transcription is marked with red dot.

3.1.3. Screening for positive transformants

After successful transformation of *N. magadii* L11-pKSII-ΔORF46(*soj*) with novobiocin cassette in forward and reverse direction (ΔORF46(*soj*)-NovR-F and R) in *N. magadii* L11, screening for transformants which no longer contain ORF46 was achieved by analytical PCR. A set of primers binding to the sequence of the novobiocin resistance cassette (Nov-9 and Nov-12) as well as primer specific for 5' end (OR-I) and primers which detect 3' end (SC-7 and SC-21) were used. Schematic representation of primer binding sites is shown in figure 18.

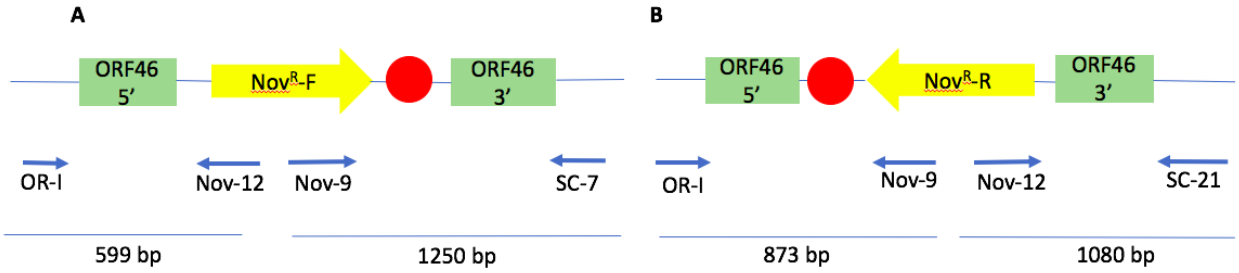

Figure 18. Schematic representation of primer binding sites for screening of double crossover of *N. magadii* L11-ΔORF46(*soj*)-NovR-F and *N. magadii* L11-ΔORF46(*soj*)-NovR-R. Primers Nov-9 and Nov-12 were used for screening of the presence of novobiocin cassette. **A** Screening for successful homologous recombination of novobiocin cassette in forward orientation was achieved by analytical PCR using primers OR-I and SC-7 for the up- and downstream region whereas **B** for screening of novobiocin cassette in reverse orientation, primers OR-I and Nov-9 were used to screen 5' end and Nov-12 together with SC-21 were used for screening of the 3' end.

Screening for double crossover of *N. magadii* L11-ΔORF46(*soj*)-NovR-F yielded positive results showing that the novobiocin resistance cassette was successfully inserted (Fig. 19). PCR products matched the expected fragment sizes. Signal at 1250 bp can be detected for 5' crossover, while screening for 3' crossover yielded a band of 599 bp. The amplification products of 1250 bp as well as 599 bp could be detected for culture no. 2 (Fig. 19, lanes 5 and 6) and for culture no. 3 (Fig. 19, lanes 7 and 8). Thus, a *N. magadii* L11-ΔORF46(*soj*)-NovR-F mutants could be identified.

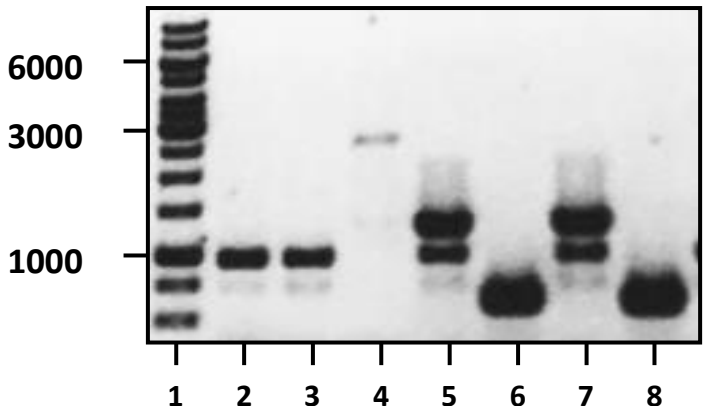

Figure 19. Screening for double crossover of *N. magadii* L11-ΔORF46(*soj*)-NovR-F. Lane 1: 1 kb ladder, lane 2: *N. magadii* L11, lanes 3-8: three different cultures after transformation of *N. magadii* L11-

ΔORF46(*soj*)-NovR-F into plasmid pKSII. Lanes 3, 4: culture no. 1, lanes 5, 6: culture no. 2, lanes 7, 8: culture no. 3, lanes 3, 5, 7: 3' crossover, lanes 4, 6, 8: 5' crossover. Primers used for screening of 5' end: OR-I and Nov-12. 3' end was amplified with primers SC-7 and Nov-9.

Screening for *N. magadii* L11-ΔORF46(*soj*)-NovR-R was achieved by analytical PCR with primers OR-I and Nov-9 for 5' end and SC-21 and Nov-12 for 3' end. One positive transformant with inserted novobiocin resistance cassette could be detected. 5' crossover of 873 bp as well as 3' crossover of size 1080 bp were successfully detected (Fig. 20).

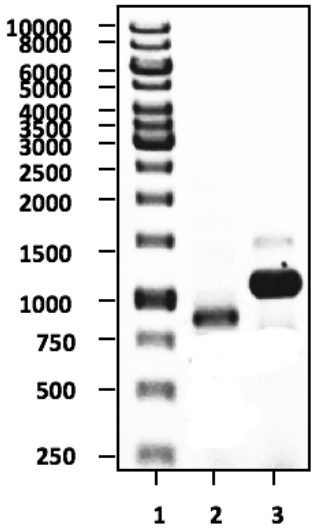

Figure 20. Screening for double crossover of *N. magadii* L11-ΔORF46(*soj*)-NovR-R. Lane 1: 1 kb ladder, lane 2: 5' crossover amplified with primers OR-I and Nov-9 resulting in 873 bp. Lane 3: 3' crossover screened with primers SC-21 and Nov-12 yielding a fragment of 1080 bp.

3.1.4. Homogenization of *N. magadii* L11-ΔORF46(*soj*)-NovR-R

As mentioned before, *N. magadii* L11 contains up to 50 copies of chromosomal and ϕCh1 DNA. Therefore, the majority of viral DNA copies still contain ORF46. After transformation with the plasmid pKSII-ΔORF46(*soj*)-NovR-R into *N. magadii* L11, it was essential homogenize the strains. Due to time limit, only strain *N. magadii* L11-ΔORF46(*soj*)-NovR-R was homogenized. Positive

transformant was incubated at 37°C until lysis occurred. Homogenization was performed by infecting L13 with virus particles of deleted strains (see 2.2.4) and plating on rich medium agar plates with novobiocin. The plates were incubated at 42°C. Afterwards colonies were grown into rich medium and tested for the presence of wild type ORF46 by analytical PCR. Primers Soj-3 and Soj-Kpn anneal to ORF46 which encodes Soj protein and result in the fragment of size 1166 bp. Fragment with the size of 1166 bp can be detected in the wild type *N. magadii* L11 meaning it contains ORF46 (Fig. 21, lane 5). Two of the tested colonies after infection of *N. magadii* L13 with showed an amplification product of 3100 bp (Fig. 21, lane 2 and 3). No signal at 1166 bp can be detected for *N. magadii* L11 ΔORF46(*soj*)-NovR-R clone 1 and 5 (Fig. 21, lanes 2 and 3) confirming that ORF46 was successfully deleted. *N. magadii* L13 is not infected by ϕCh1. Therefore, it lacks ORF46 and no signal could be observed (Fig. 21, lane 4).

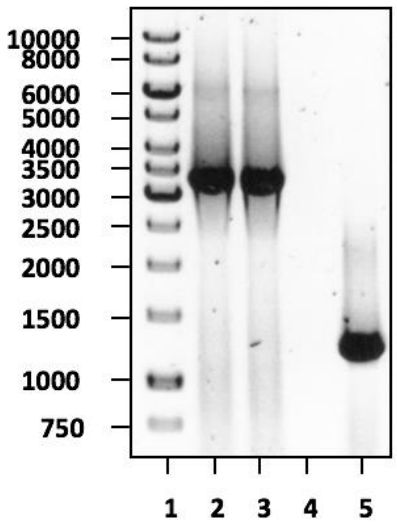

Figure 21. Verification of homogenized *N. magadii* L11-ΔORF46(*soj*)-NovR-R clone 1 and 5. Lane 1: 1 kb DNA ladder, lane 2: *N. magadii* L11-ΔORF46(*soj*)-NovR-R clone 1, lane 3: *N. magadii* L11-ΔORF46(*soj*)-NovR-R clone 5, lane 4: *N. magadii* L13, lane 5: *N. magadii* L11. Analytical PCR was performed using templates from *N. magadii* L11-ΔORF46(*soj*)-NovR-R clone 1 and 5 as well as from *N. magadii* L13 and *N. magadii* L11 that served as controls. Samples were amplified with primers Soj-3 and Soj-Kpn to determine the presence of wild type ϕCh1.

3.1.5. Confirmation of homozygous *N. magadii* L11-ΔORF46(*soj*)-NovR-R with Southern Blot

Considering that PCR analysis can occasionally yield erroneous results, successful deletion and homogenization of *soj* from the wild type ϕCh1 had to be further confirmed. In order to detect specific DNA sequences in the probes, a Southern blot was performed. Therefore, DNA from ϕCh1-ΔORF46(*soj*)-NovR-R clone 5 was isolated (see 2.2.5.2) from purified viral particles (see 2.2.5.1) and restricted with *BamHI* together with the wild type ϕCh1. Next, restricted probes were separated on a 0.8 % agarose gel and transferred onto a nylon membrane. Further, the samples were hybridized with probes specifically designed for 5' and 3' end. The upstream region (5') was amplified with primers 44-B and Δsoj-2 resulting in a fragment with size of 1700 bp whereas the downstream region (3') was synthesized using primers Δsoj-3 and Δsoj-4 which yield a fragment of 750 bp. For both PCR reactions, wild type ϕCh1 and biotinylated dUTPs were used (see 2.2.6).

Figure 22 depicts specifically designated probes for hybridization and expected fragments' sizes. Probes specific for the upstream region (5') of wild type ϕCh1 should detect two fragments of 1950 bp and 780 bp. Detection of the downstream region (3') yields one fragment of size 3059 bp. However, since deletion mutant *N. magadii* L11-ΔORF46(*soj*)-NovR-R contains novobiocin resistance cassette, detection of the 5' end should result in 5641 bp in addition to 1950 bp whereas hybridization with 3' end should yield one big fragment of 5641 bp (Fig. 22).

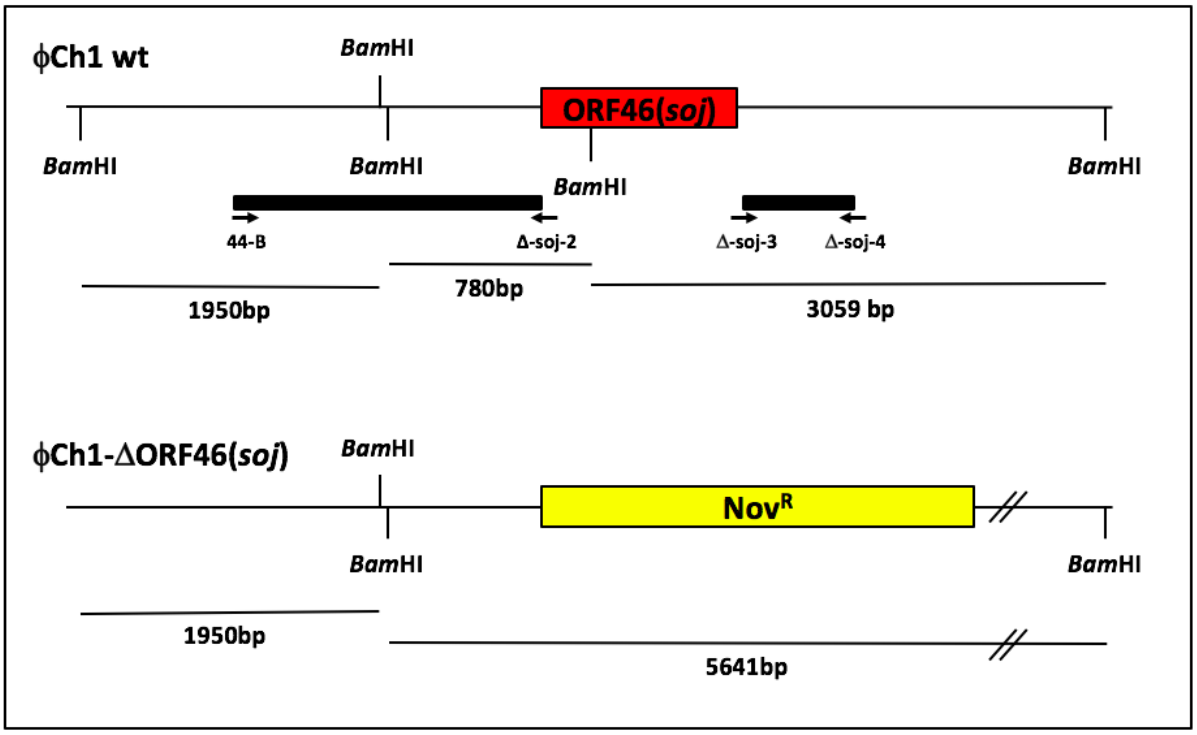

Figure 22. Schematic representation of probes hybridization for Southern Blot. Wild type ϕCh1 and ϕCh1-ΔORF46(*soj*)-NovR-R were restricted with *BamHI*. The probe for the upstream region (5') was synthesized with primers 44-B and Δsoj-2 whereas the downstream region (3') was amplified with Δsoj-3 and Δsoj-4 primers. Construction of both probes was achieved by PCR using ϕCh1 as a template and biotinylated dUTP. Detection of the 5' end of wt ϕCh1 should result in two fragments of sizes 1950 bp and 780 bp. 3' detection should yield a fragment of 3059 bp. Since there is novobiocin resistance cassette inserted in ϕCh1-ΔORF46(*soj*)-NovR-R, 3' detection of this clone should result in one fragment of 5641 bp. 5' detection of ϕCh1-ΔORF46(*soj*)-NovR-R yields fragments with size of 1950 bp and 5641 bp. The drawing is not to scale.

Southern blot analyses confirmed the expected results (Fig. 23). Figure 23B shows the signals for wt ϕCh1 and ϕCh1-ΔORF46(*soj*)-NovR-R which are hybridized with the probe for 5' end. Two bands for wt ϕCh1 of 780 bp and 1950 bp can be observed. Due to deletion of ORF46 and insertion of the novobiocin resistance cassette in the strain ϕCh1-ΔORF46(*soj*)-NovR-R, a large fragment of 5641 bp in addition to 1950 bp can be observed when the probes were hybridized for 5' end. Furthermore, Figure 23C depicts hybridization of 3' end of wt ϕCh1 and ϕCh1-

ΔORF46(*soj*)-NovR-R. Hybridization signal for 3' end of wt ϕCh1 yielded a fragment of 3059 bp while ϕCh1-ΔORF46(*soj*)-NovR-R resulted in fragment of 5641 bp as a consequence of the inserted novobiocin resistance cassette in reverse direction. Here, only the results of ϕCh1 ΔORF46(*soj*)-NovR-R clone no. 5 are shown. Finally, we were able to certainly verify a successful deletion of ORF46 from the wt ϕCh1.

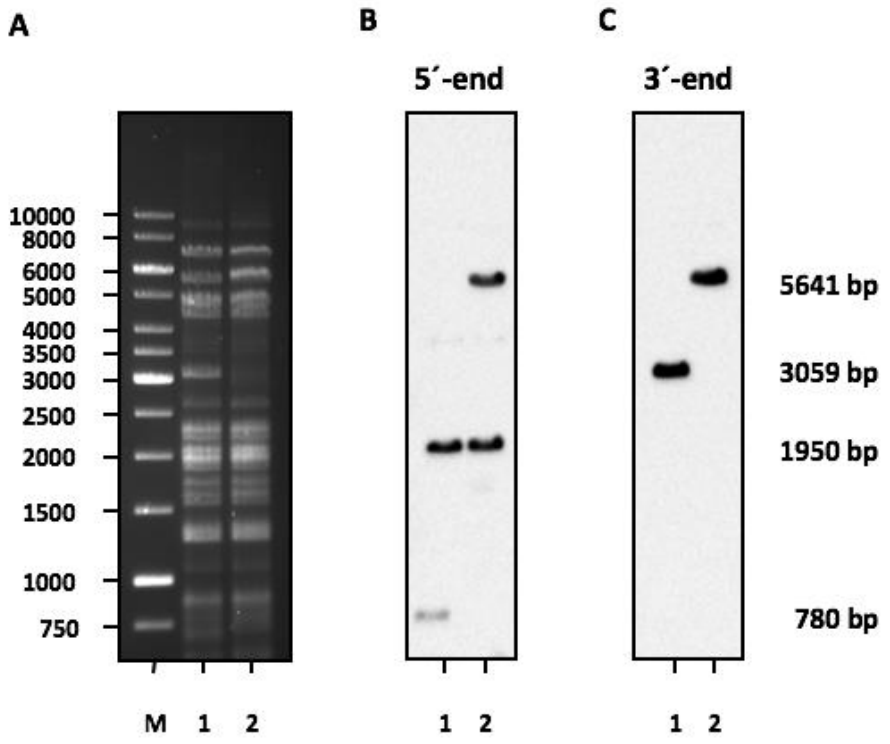

Figure 23. Southern Blot analysis of wild type ϕCh1 and ϕCh1-ΔORF46(*soj*)-NovR-R clone 5. A Restriction of wt ϕCh1 (lane 1) and ϕCh1-ΔORF46(*soj*)-NovR-R clone 5 (lane 2) with *BamHI* applied on 0.8 % agarose gel. Next, the samples were blotted on a nylon membrane and hybridized with 5' and 3' specific probes. **B** Hybridization with the 5' probe. Lane 1: wt ϕCh1, lane 2: ϕCh1-ΔORF46(*soj*)-NovR-R clone no. 5 **C** Hybridization with the 3' probe. Lane 1: wt ϕCh1, lane 2: ϕCh1-ΔORF46(*soj*)-NovR-R clone no. 5. 1kb DNA ladder is indicated on the left (M). Expected fragment sizes are indicated on the right.

3.1.6. Growth kinetics analysis of *N. magadii* L11 and *N. magadii* L11-ΔORF46(*soj*)-NovR-R

For further analysis of the soj deletion on *N. magadii* L11, growth kinetics of deletion strain *N. magadii* L11-ΔORF46(*soj*)-NovR-R together with *N. magadii* L11 were investigated. Cultures were inoculated in rich medium at OD_{600} of 0.1 and incubated at 37°C for 6 days.

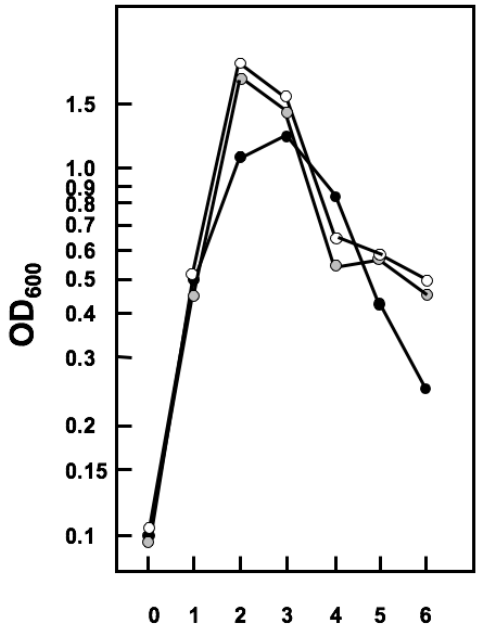

Figure 24. Growth kinetics analysis of *N. magadii* L11 and *N. magadii* L11-ΔORF46(*soj*)-NovR-R clone 1 and 5. *N. magadii* L11 (black circle), *N. magadii* L11-ΔORF46(*soj*)-NovR-R clone 1 (white circle) and *N. magadii* L11-ΔORF46(*soj*)-NovR-R clone 5 (grey circle) were investigated for their growth and lysis behavior. The strains were inoculated in rich medium and grown at 37°C with agitation. Optical density was measured every day at 600 nm.

As shown in figure 24, *N. magadii* L11 strain lysed on day 3-4 after inoculation whereas onset of lysis of *N. magadii* L11-ΔORF46(*soj*)-NovR-R clone 1 and 5 occurred one day earlier. Lysis of strains lacking ORF46 started on day 2-3. Both clones of *N. magadii* L11-ΔORF46(*soj*)-NovR-R showed similar behavior in their growth and lysis as hypothesized.

3.1.7. Expression of ORF46 (*soj*) in *N. magadii* L11 and *N. magadii* L11-ΔORF46(*soj*)-NovR-R

Effect of ϕCh1 ORF46 (*soj*) deletion was further studied through expression of *soj* in *N. magadii* L11 and *N. magadii* L11-ΔORF46(*soj*)-NovR-R clone 5. Strains were inoculated in rich medium and grown at 37°C for 5 days. Afterwards, crude protein extracts (see 2.2.7.1) were prepared, applied on 12 % SDS-PAGE gel and stained with Coomassie Brilliant Blue dye to determine their concentration (Fig. 25).

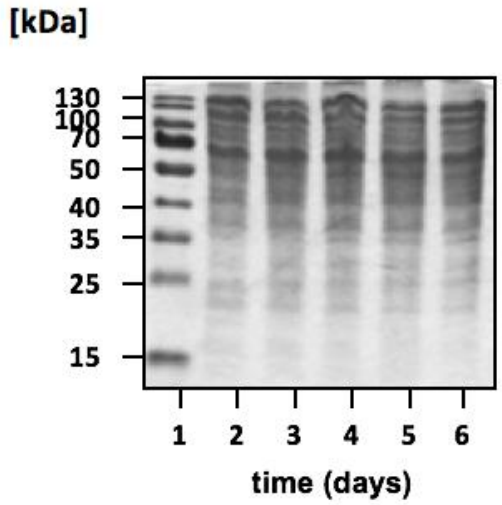

Figure 25. Expression of *N. magadii* L11 at different time points stained with Coomassie Brilliant Blue Dye. Lane 1: prestained protein ladder, lanes 2-6: crude extracts prepared each day. *N. magadii* L11 was inoculated at OD_{600} of 0.1 and grown for 5 days at 37°C. Every day crude extracts were prepared. Afterwards, they were applied on 12 % SDS-PAGE gel and stained with Coomassie Briliant Blue Dye to determine the concentration of the samples which are later used for Western blots.

Expression of ORF46 was analyzed by Western blot using α-Soj antibody (1:250) (see 2.1.10).

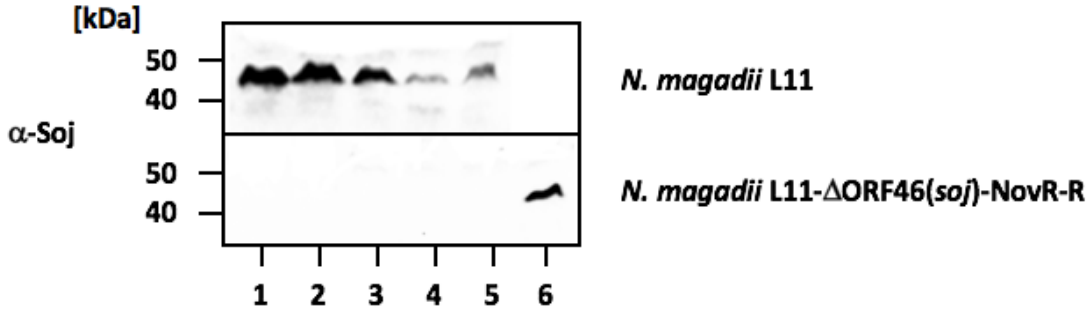

Figure 26. Expression of ORF46 in *N. magadii* L11 and *N. magadii* L11 ΔORF46(*soj*)-NovR-R. Strains were grown at 37°C for 5 days. Crude extracts were prepared each day and applied on 12 % SDS-PAGE gel. Afterwards, samples were transferred onto a nitrocellulose membrane and detected with a α-Soj antibody (1:250). Lanes 1-5: samples taken every day from day 1 to 5. Lane 6- *N. magadii* L11 as a control.

Protein Soj has a size of approximately 45 kDa. A clear signal at around 45 kDa can be observed in figure 26, demonstrating a clear expression of *soj* in wild type *N. magadii* L11 during all 5 days after inoculation of the strain. In contrast, the protein Soj in the strain *N. magadii* L11 ΔORF46(*soj*)-NovR-R clone 5 cannot be detectable, proving that ORF46 which encodes protein Soj has indeed been deleted.

3.1.8. Virus titer analysis

Earlier onset of lysis of *N. magadii* L11-ΔORF46(*soj*)-NovR-R which lacks ORF46 (Fig. 27) led to the investigation of number of virus particles released by the same strain. Virus titer analysis was performed by infecting *N. magadii* L13 with the supernatants of *N. magadii* L11-ΔORF46(*soj*)-NovR-R.

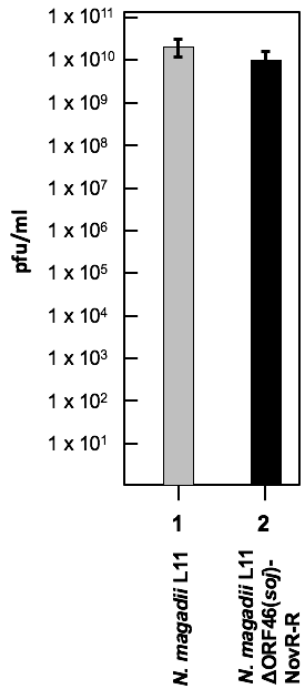

Figure 27. Virus titer analysis of strains *N. magadii* L11 and *N. magadii* L11-ΔORF46(*soj*)-NovR-R. Lane 1: *N. magadii* L11; lane 2: *N. magadii* L11-ΔORF46(*soj*)-NovR-R. Supernatants of the samples which contain virus particles were taken at day 5.

Figure 27 illustrates the number of released virus particles of *N. magadii* L11 that served as a control and *N. magadii* L11-ΔORF46(*soj*)-NovR-R. Both strains have a magnitude at around 10, which represents the number of released virus particles as determined by virus titer analysis. Thus, despite the difference in onset of lysis, there seems to be no alterations in lysis kinetics.

3.1.9. Expression of ORF11 in *N. magadii* L11 and *N. magadii* L11-ΔORF46(*soj*)-NovR-R

Further examination of deletion of ϕCh1 ORF46 on *N. magadii* L11 and development of ϕCh1 was achieved through investigation of expression of major capsid protein E encoded by ORF11. Crude protein extracts of *N. magadii* L11 and *N. magadii* L11-ΔORF46(*soj*)-NovR-R clone 5 were

prepared (see 2.2.7.1). The expression of protein E was detected with Western blot using α-E antibody (1:2500) (see 2.1.10).

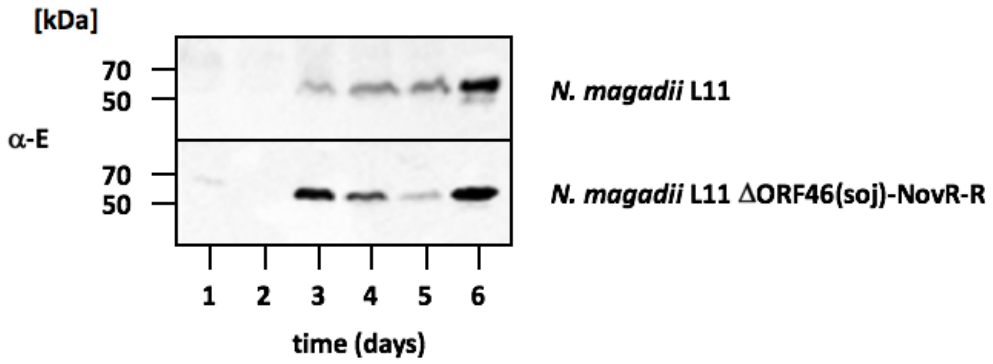

Figure 28. Expression of ORF11 in *N. magadii* L11 and *N. magadii* L11-ΔORF46(soj)-NovR-R. Crude extracts were prepared from *N. magadii* L11 and *N. magadii* L11-ΔORF46(*soj*)-NovR-R clone 5 which are then separated on 12 % SDS PAGE gel. Expression of protein E was detected with α-E antibody (1:2500) by Western blot. Lane 1-5: samples taken from day 1 to 5; lane 6: protein E as a control.

As previously shown, onset of lysis of *N. magadii* L11-ΔORF46(*soj*)-NovR-R clone 5 occurred 24 hours earlier in comparison to the wild type *N. magadii* L11. However, the expression of major capsid gene E in both strains was first detected on day 3 when lysis of *N. magadii* L11 occurred. ORF11 expression in *N. magadii* L11 seems to be increasing with time after inoculation whereas in deletion mutant, protein E is the strongest expressed on day 3 (Fig. 28). Furthermore, the intensity of protein E expression in clone 1 of *N. magadii* L11-ΔORF46(*soj*)-NovR-R additionally to clone 5 appear to be the same (data not shown).

3.1.10. Discussion

In order to gain a clearer perception about the virus ϕCh1 and its genome organization, one part of this study focused on ϕCh1 ORF46 that encodes the protein Soj. Previous research indicated that Soj is presumably involved in plasmid partitioning process. Additionally, Soj might conceivably play a role in the stability of the plasmid pNB102. In the absence of Soj, the plasmid pNB102 was stable whereas the addition of Soj led to a rapid loss of the plasmid pNB102 in *N. magadii* L13 (Hofbauer, 2015). To further elucidate Soj's function, a mutant strain which lacks ORF46 was constructed. Considering that *N. magadii* contains up to 50 copies of chromosomal and ϕCh1 DNA, homogenization of the positive clone lacking ORF46 was essential. Screening for the clone in which ORF46 was exchanged with the novobiocin resistance cassette in reverse orientation was done by analytical PCR. Due to erroneous results of PCR analyses, additional confirmation of homogenized deletion mutant was performed with Southern blot which faithfully approved deletion of ORF46. Finally, further characterization of ORF46 could be accomplished after successful construction of deletion mutant *N. magadii* L11-ΔORF46(*soj*)-NovR-R.

First, growth curve analysis demonstrated that the onset of lysis of *N. magadii* L11-ΔORF46(*soj*)-NovR-R started one day earlier in comparison to the wild type *N. magadii* L11 indicating a clear influence on the regulation of ϕCh1 life cycle. In contrast, virus titer analysis did not show significant alterations in the number of released virus particles in two comparable strains suggesting that ORF46 indeed has unique effect on the onset of lysis.

Next, analyses of *soj* expression by Western blot could not detect the protein Soj in the mutant strain lacking ORF46 which confirmed our expectations whereas in the wild type there was an early *soj* gene expression which reduces over time. One possible explanation could be that the loss of Soj induces the loss of the circular intermediate, which could be a potential target for Soj. Therefore, the number of virus producing cells might be reduced which should lead to the reduction or loss of virus progeny. Surprisingly, the expression of ORF11, encoding the major capsid protein E started on day 3 in both strains. In the wild type *N. magadii* L11, lysis occurred

on day 3 and ORF11 expression is increased over time. Despite the earlier lysis of the deletion mutant strain, ORF11 expression was detected on day 3 as well. However, the expression of ORF11 is decreased over the time.

3.2. ORF49

Aim

There have been indications that ORF49 is involved in gene regulation of ϕCh1 by acting as a putative repressor encoding gene. The insertion of 223 bp into ORF49 of ϕCh1 leads to an earlier onset of lysis of the lysogenic strain *N. magadii* L11-1 (Iro *et al*., 2007). In addition, N. *magadii* L13 (pRo-5-ORF49), carrying ORF49 on plasmid pRo-5, showed a reduced infectivity of ϕCh1 compared to the wild type strain (Reiter, 2010). Regarding this, the aim of this study was to construct *N. magadii* L11 deletion mutants which lack ORF49 in order to further investigate the function of ORF49 in *N. magadii* L11. Therefore, ORF49 should be deleted from the genome of ϕCh1.

3.2.1. Construction of pKSII-ΔORF49-NovR-F and pKSII-ΔORF49-NovR-R

The plasmids were constructed containing a novobiocin resistance cassette in forward and reverse orientation flanked by an upstream and downstream region of ϕCh1 ORF49 (see 2.2.8.1). Replacement of ϕCh1 ORF49 with novobiocin resistance cassette should occur via homologous recombination. Fragments were cloned into plasmid pBlueScript II KS + (pKSII+) which lacks an applicable origin of replication for *N. magadii* (Fig. 29). Therefore, after successful homologous recombination, pKSII+ is not able to replicate autonomously in *N. magadii*. The constructs were transformed in *N. magadii* L11. After successful transformation, screening for positive transformants occurred and they were subsequently homogenized.

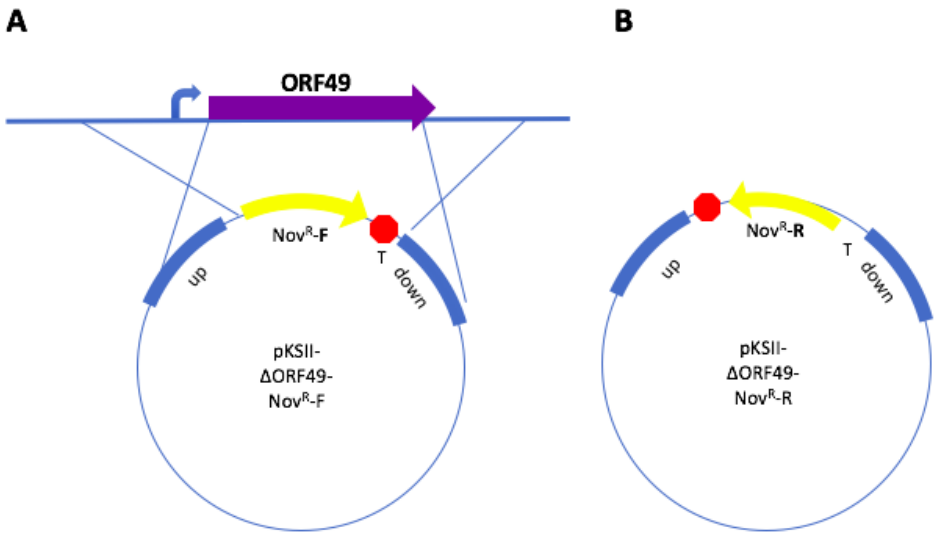

Figure 29. Schematic representation of constructed ORF49 deletion mutants. Blue arrow represents the ORF49 promoter. Two orientations of novobiocin resistance cassette (**A**) forward and **B**) reverse) are represented as yellow arrows. Flanking regions marked blue are essential for homologous recombination whereas red dot depicts a terminator sequence.

3.2.2. Screening for positive transformants

After successful transformation of plasmids pKSII-ΔORF49-NovR-F and pKSII-ΔORF49-NovR-R into *N. magadii* L11 (*N. magadii* L11-pKSII-ΔORF49-NovR-F and *N. magadii* L11-pKSII-ΔORF49-NovR-R), screening for double crossover of positive transformants was done via analytical PCR. Deletion of ORF49 and its replacement with novobiocin resistance cassette successfully occurs only in case of a double crossover event. Therefore, screening for 5' and 3' end of the transformants was essential. Primers Nov-6, Nov-9, Nov-12 and Nov-13, which anneal to the novobiocin resistance cassette were chosen as well as 49-5-en for 5' end and 49-3-en which binds to the 3' end of the sequences used for the recombination events (Fig. 30).

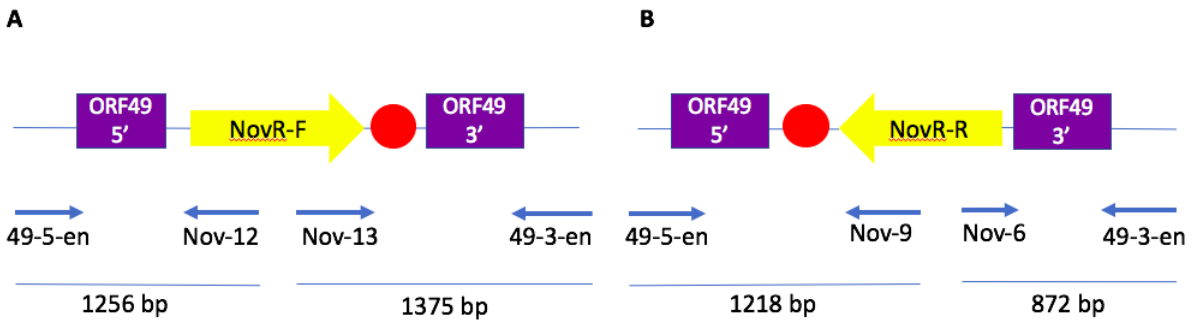

Figure 30. Schematic representation of primer binding sites for screening of double crossover. Primer 49-5-en was used to screen for 5' end whereas 49-3-en detected 3' end. Depending on the orientation of novobiocin resistance cassette, primers Nov-12 and Nov-13 (forward direction) and Nov-6 and Nov-9 (reverse direction) were used. **A)** ORF49 deletion mutant with novobiocin resistance cassette in forward direction **B)** ORF49 deletion mutant with novobiocin resistance cassette in reverse direction.

30 cultures were tested (Fig. 31 indicates 9 cultures), obtained after transformation of *N. magadii* L11 with plasmid pKSII-ΔORF49-NovR-F, were used for analysis of a double crossover (Fig. 31). Each culture was tested by PCR with primers 49-5-en and Nov-12 to verify 5' crossover. Primer Nov-12 is located within the novobiocin resistance cassette whereas 49-5-en is located upstream of the sequence used for the recombination at the 5'-site of ORF49. The expected fragment has a size of 1256 bp. As shown in figure 31A, clones no. 3, 6, and 8 showed a fragment of the calculated size (lanes 4, 7, and 9). All other cultures showed only unspecific amplification products. In order to determine the 3' crossover all cultures were used for PCR analyses with primers Nov-13 and 49-3-en. Primer 49-3-en binds to the sequence downstream of the recombination sequence, whereas Nov-13 is located within the novobiocin resistance gene (Fig. 30). A positive PCR product with a length of 1375 bp could be obtained for cultures 3, 6, and 8 (Fig. 31B, lanes 4, 7, and 9). Therefore, cultures 3, 6, and 8 contained a double crossover and were used for further investigations.

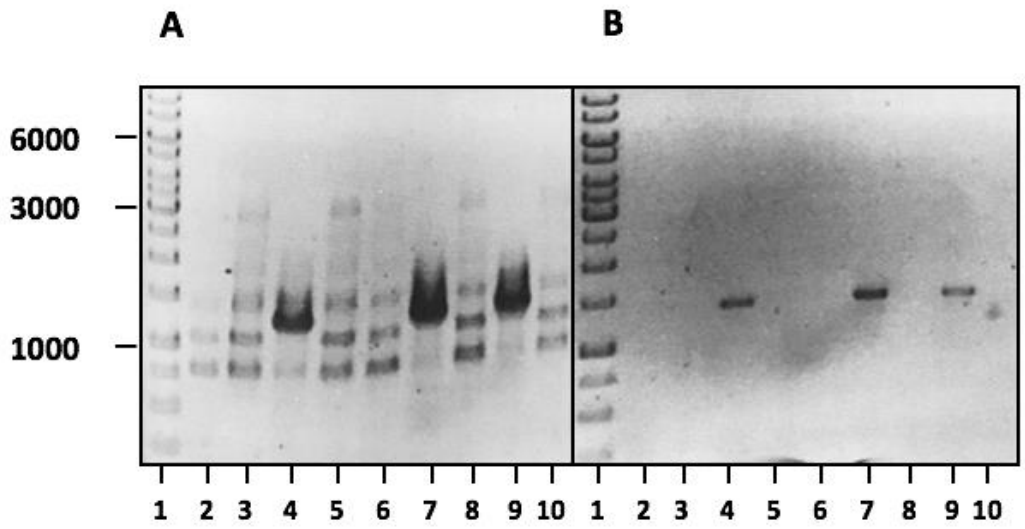

Figure 31. Double crossover screening of *N. magadii* L11-ΔORF49-NovR-F. A 5' crossover, lane 1: 1 kb ladder, lanes 2-10: 1 to 9 clones of *N. magadii* L11-ΔORF49-NovR-F transformed into *N. magadii* L11 **B** 3' crossover, lane 1: 1 kb ladder, lanes 2-10: 1 to 9 clones of *N. magadii* L11-ΔORF49-NovR-F transformed into *N. magadii* L11. 5' end was amplified with primers 49-5-en and Nov-12 while primers 49-3-en and Nov-13 were used for screening of 3' crossover.

Screening for the integration of *N. magadii* L11-ΔORF49-NovR-R was performed by analytical PCR with primers 49-3-en and Nov-6 for 3' end and 49-5-en and Nov-9 for 5' end. One clone was detected with an expected double crossover (Fig. 32, lanes 12 and 13). Here, an amplification products of 872 bp for the 3' crossover and 1218 bp for 5' crossover could be detected.

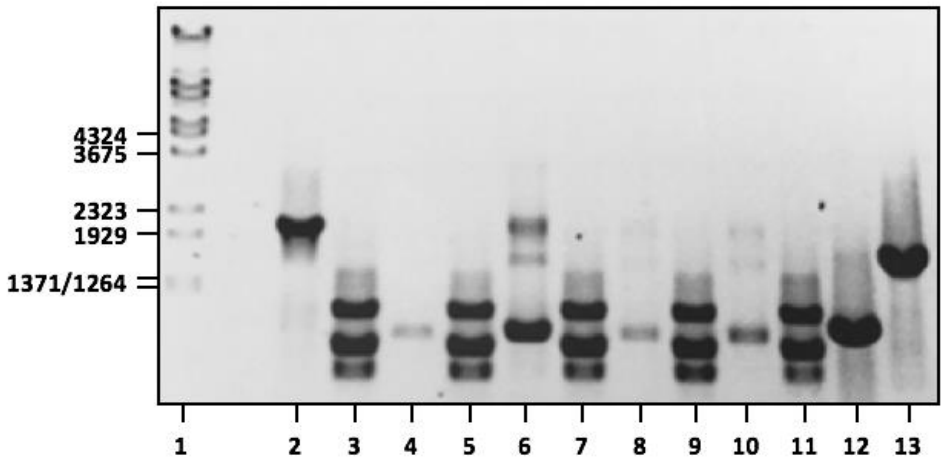

Figure 32. Double crossover screening of *N. magadii* L11-ΔORF49-NovR-R. Lane 1: λ BstEII ladder, lanes 2, 4, 6, 8, 10, 12: 3' crossover amplified with primers 49-3-en and Nov-6, lanes 3, 5, 7, 9, 11, 13: 5' crossover screened using primers 49-5-en and Nov-9.

3.2.3. Homogenization of *N. magadii* L11-ΔORF49-NovR-F

N. magadii L11 contains up to 50 copies of both chromosomal and ϕCh1 DNA (Breuert *et al*., 2006). Therefore, homogenization of cloned mutants was essential to ensure that wild type ϕCh1 ORF49 is absent in every copy of viral DNA. There are various methods for performing homogenization. In this study, the strain *N. magadii* L13 was infected with virus particles containing deleted mutants which should result in a homozygous strain. Theoretically, one virus particle is sufficient for infection of *N. magadii* L13. A positive tested culture was incubated at 37°C until lysis occurred. Next, a *N. magadii* L13 culture was infected with the viral lysate and plated on rich medium agar plates containing novobiocin. This approach ensured the growth of cells lacking wild type ORF49. For detailed description of homogenization method see section 2.2.4.

Next, single colonies were tested for successful deletion of ORF49. Due to time limit, only deletion mutant *N. magadii* L11-ΔORF49-NovR-F was homogenized. First, the absence of wild type ϕCh1 DNA was tested using primers ORF49-Nde and ORF49-Bam which screen for coding

region of ORF49 including overhangs. Next, primer named ORF49-Kpn that is located in the external region of the cloned fragment was used together with primer ORF49-Bam for further confirmation of the absence of the wild type ORF49. *N. magadii* L11 served as a negative control. Both PCR reactions were performed with 50 cycles to ensure deletion of every copy of ORF49 (Fig. 33). PCR analyses proved that *N. magadii* L11-ΔORF49-NovR-F was successfully homogenized. As shown in figure 33, wild type L11 was detected in both PCR reactions using previously described primers. Primers ORF49-Nde and ORF49-Bam yielded the size of 374 bp for L11 whereas 49-Kpn and 49-Bam produced 533 bp long L11 fragment. Both PCR reactions could not detect ORF49 in our putative *N. magadii* L11-ΔORF49-NovR-F clone indicating that ORF49 has indeed been deleted.

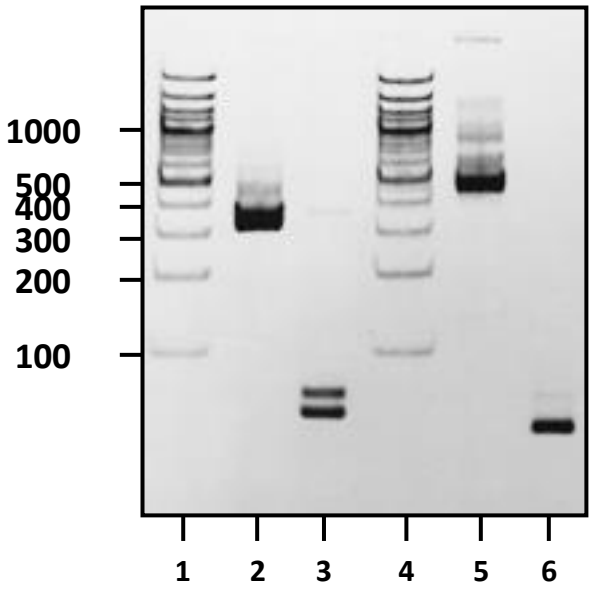

Figure 33. Verifcation of homogenized *N. magadii* L11-ΔORF49-NovR-F. Samples were separated on an 6 % PAA gel and stained with ethidium bromide Lanes 1, 4: 100 bp ladder, lanes 2, 5: *N. magadii* L11, lanes 3, 6: putative homogenized *N. magadii* L11-ΔORF49-NovR-F. Analytical PCR was performed using templates from *N. magadii* L11-ΔORF49-NovR-F as well as from L11 that served as control. First, samples were amplified with primers ORF49-Nde and ORF49-Bam to verify the presence of wild type ϕCh1 which resulted in fragment of 374 bp. Further absence of wt ORF49 was confirmed with primers ORF49-Kpn and ORF49-Bam yielding a signal at 533 bp.

To further confirm homogenization of *N. magadii* L11-ΔORF49-NovR-F, another PCR with 50 cycles was prepared using primers ORF49-Kpn and Δ53-1. PCR products were applied on 0.8 % agarose. *N. magadii* L11 was used as a negative control yielding the size of 760 bp whereas putative homogenized *N. magadii* L11-ΔORF49-NovR-F resulted in 2967 bp as shown in figure 34, lane 3. Therefore, it could be additionally confirmed that *N. magadii* L11-ΔORF49-NovR-F was successfully homogenized as no wild type fragment with the size of 760 bp could be detected (Fig. 34, lane 3).

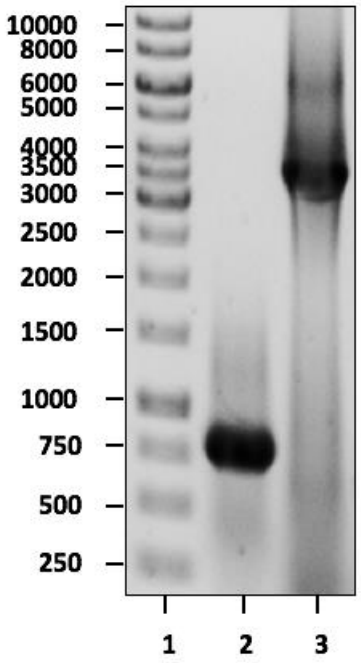

Figure 34. Verification of homogenized *N. magadii* L11-ΔORF49-NovR-F. Samples were separated on an 0.8 % agarose gel and stained with ethidium bromide. Lane 1: 1 kb ladder, lane 2: *N. magadii* L11, lane 3: homogenized *N. magadii* L11-ΔORF49-NovR-F. Analytical PCR was performed using a template from *N. magadii* L11-ΔORF49-NovR-F as well as from *N. magadii* L11 that served as control. Samples were amplified with primers ORF49-Kpn and Δ53-1.

3.2.4. Growth kinetics analysis

Investigation of the effect of ORF49 deletion on the phenotype of *N. magadii* L11 included a growth curve analysis. Previous studies showed that lysogenic strain L11 carrying a mutant ϕCh1-1 lysed earlier in comparison to the wild type *N. magadii* L11 (Iro et al., 2007). Therefore, in this study, the growth and lysis behavior of homogenized strain *N. magadii* L11-ΔORF49-NovR-F inoculated with and without novobiocin was compared to the wild type *N. magadii* L11 which carries the virus ϕCh1.

Strains *N. magadii* L11 and *N. magadii* L11-ΔORF49-NovR-F were inoculated in rich medium with and without antibiotic and grown at 37°C with agitation. Optical density was measured every day at 600 nm (Fig. 35).

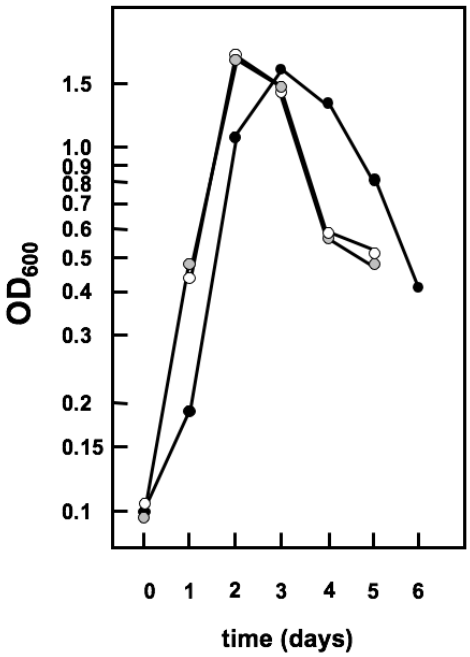

Figure 35. Growth kinetics analysis of *N. magadii* L11 and *N. magadii* L11-ΔORF49-NovR-F with novobiocin and *N. magadii* L11-ΔORF49-NovR-F without novobiocin. *N. magadii* L11 (black circle), *N. magadii* L11-ΔORF49-NovR-R with novobiocin (white circle) and *N. magadii* L11-ΔORF49-NovR-R without novobiocin (grey circle) were investigated for their growth and lysis behavior. The strains were inoculated in rich medium and grown at 37°C with agitation. Optical density was measured every day at 600 nm.

Figure 35 outlines that the onset of lysis of strains *N. magadii* L11-ΔORF49-NovR-F inoculated with and without antibiotic novobiocin started on day 2-3 whereas the wild type L11 strain lysed on day 3-4. However, the strain *N. magadii* L11-ΔORF49-NovR-F grown with novobiocin did not show significant difference in growth behavior compared to the same strain *N. magadii* L11-ΔORF49-NovR-F grown in the absence of the novobiocin. Earlier onset of lysis of deletion mutant strain confirmed that ORF49 is involved in gene regulation of ϕCh1.

3.2.5. Expression of ORF11 in *N. magadii* L11 and *N. magadii* L11-ΔORF49-NovR-F

Examination of the effect of ϕCh1 ORF49 on gene expression of ϕCh1 and the expression of ORF11, encoding the major capsid protein E was achieved by Western Blot analyses.

First, the protein concentrations of *N. magadii* L11 were determined by Coomassie staining (see Fig. 25). Next, the expression of ORF11 in strains *N. magadii* L11 and *N. magadii* L11-ΔORF49-NovR-F was detected with α-E antibody by Western blot.

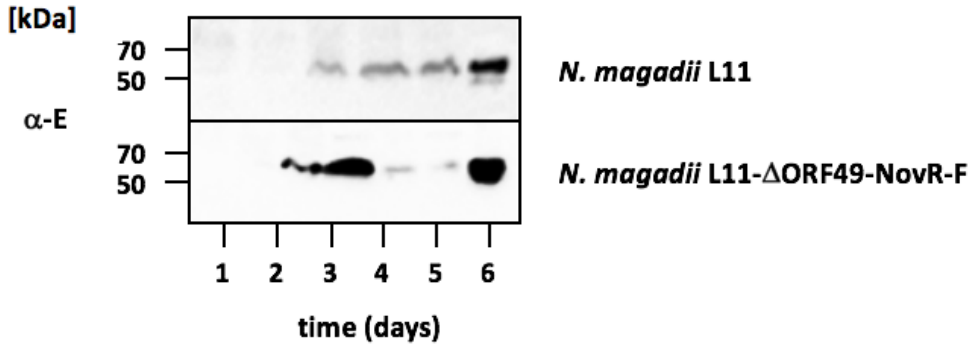

Figure 36. Expression of ORF11 in *N. magadii* L11 and *N. magadii* L11-ΔORF49-NovR-F. Lanes 1-5: protein crude extracts prepared every day from day 1-5, lane 6: protein E control. Crude extracts were prepared from strain *N. magadii* L11 and *N. magadii* L11-ΔORF49-NovR-F at different time points (see 2.2.7.1) and applied on 12 % SDS-PAGE. Samples were detected with α-E antibody (1:2500).

Expression of major capsid protein E which is encoded by ORF11 started on day 3 in the wild type strain *N. magadii* L11, while in the strain *N. magadii* L11-ΔORF49-NovR-F an earlier expression of protein E could be detected (Fig. 36). Here, the first detectable signal was seen in lane 2 of figure 36, representing the sample taken at day 2 (see figure 35 for details). In both strains, protein E is expressed as lysis occurs.

3.2.6. Discussion

Over the past 20 years, different open reading frames (ORFs) of *N. magadii* virus ϕCh1 were investigated. Very few studies focused on ORF49 which was claimed to be a possible regulator of the ϕCh1 life cycle. Evidence for the importance of ORF49 for the ϕCh1 lytic cycle is shown by the fact that duplication of the 5' part of ORF49 triggers an earlier onset of lysis and is rather unstable over the time having tendency to return into the wild type. In addition to the ORF49, a study in 2007 identified another putative repressor encoding gene ORF48 (*rep*), which is arranged in to a head to head constellation with ORF49 and shows sequence similarities to putative repressor molecules (Iro *et al*., 2007). *Rep*- in contrast to other viruses that encode repressor genes, is constitutively transcribed throughout the whole life cycle of ϕCh1. However, ORF49 is expressed when the culture enters the logarithmic growth phase. The intensity of the signal steadily increases over time. The intergenic region between ORF48 and ORF49 contains promoter/operator sequences. In *H. volcanii* it was shown that *Rep*, the gene product of ORF48, turns off the expression of ORF49. However, gene products of ORF43/44 bind to the direct repeats of *rep* and enhance transcription of ORF49 by an unknown mechanism. In this study, our goal was to gain more insights about the ORF49. Therefore, it was attempted to obtain an ORF49 deletion mutant. For this purpose, ORF49 was successfully exchanged with the novobiocin resistance cassette via homologous recombination in strain *N. magadii* L11. Due to the evidence that *N. magadii* is a polyploid organism, homogenization of the mutant strain was essential. Screening for the absence of wild type ORF49 by analytical PCR ensured a successful homogenization of *N. magadii* L11-ΔORF49-NovR-F. However, due to time constraints, only a

mutant with novobiocin resistance cassette in forward direction was homogenized. After homogenization, ORF49 was further characterized.

It was shown that deletion mutant strain *N. magadii* L11-ΔORF49-NovR-F has an earlier onset of lysis in comparison to the wild type *N. magadii* L11.

Expression of gene E encoded by ORF11 started on the same day when lysis in the wild type *N. magadii* L11. However, in the strain *N. magadii* L11-ΔORF49-NovR-F, gene E expression was detected on day 2 as the onset of lysis started on the same day. In addition, it could be observed that in the wild type strain *N. magadii* L11, expression of gene E increases with time, meaning that the cells which remain produce more protein E whereas in the deletion strain *N. magadii* L11-ΔORF49-NovR-F, the intensity of the signal is reduced over the time.

Furthermore, the expression of ORF34 as well as methyltransferase gene, located at the central part and at the 3' end of ϕCh1 should be conducted in future studies to obtain clearer insights about the function of ORF49.

3.2.7. Variants of ORF49 deletion

3.2.7.1. Aim

Given evidence that ORF49 has an influence on lysis behavior of ϕCh1 and presumably acts as a repressor encoding gene, it was of our interest to discover the parts of ORF49 which are responsible for repressor function. Therefore, different parts of ORF49 were deleted in order to gain insights about the segments essential for repressor function.

3.2.7.2. Cloning strategy

Four different deletion variants of ORF49 were constructed by PCR (see 2.2.8.2-2.2.8.5) and cloned into vector pNB102. ORF49-Δ1 and ORF49Δ2 have truncated 3' end whereas ORF49-C1 and ORF49-C2 possess truncation in the middle part. After successful cloning, positive

transformants were transformed into *N. magadii* L11. A schematic overview of ORF49 deletion mutants is shown in figure 37.

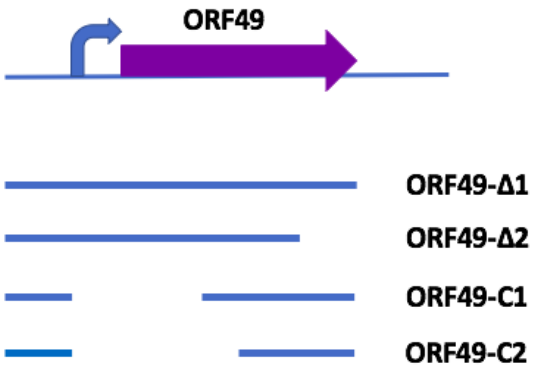

Figure 37. Schematic overview of different deletion mutants of ORF49. Blue arrow indicates promoter of ORF49. Deletion variants of ORF49 were cloned into vector pNB102 and transformed into *N. magadii* L11.

3.2.7.3. Future work

After successful transformation of ORF49 deletion mutants in *N. magadii* L11, positive transformants were found. Virus titer analysis by infecting *N. magadii* L13 with these different deletion mutants were performed. However, no significant difference in number of plaque forming units in comparison to *N. magadii* L13 control could be observed (data not shown). Therefore, putative positive deletion variants have to be sequenced for faithful confirmation of deleted variants. After positive confirmation, virus titer analysis should be performed in the future.

4. References

Albers, Sonja-Verena, and Benjamin H Meyer. 2011. “The Archaeal Cell Envelope.” *Nature Reviews. Microbiology* 9 (6):414–26. https://doi.org/10.1038/nrmicro2576.

Allers, Thorsten. 2010. “Overexpression and Purification of Halophilic Proteins in *Haloferax Volcanii*.” *Bioengineered Bugs* 1 (4):290–92. https://doi.org/10.4161/bbug.1.4.11794.

Allers, Thorsten, and Moshe Mevarech. 2005. “Archaeal Genetics — the Third Way.” *Nature Reviews Genetics* 6 (1):58–73. https://doi.org/10.1038/nrg1504.

Andrei, Adrian-Ştefan, Horia Leonard Banciu, and Aharon Oren. 2012. “Living with Salt: Metabolic and Phylogenetic Diversity of Archaea Inhabiting Saline Ecosystems.” *FEMS Microbiology Letters* 330 (1):1–9. https://doi.org/10.1111/j.1574-6968.2012.02526.x.

Baranyi, U, R Klein, W Lubitz, D H Krüger, and A Witte. 2000. “The Archaeal Halophilic Virus-Encoded Dam-like Methyltransferase M. phiCh1-I Methylates Adenine Residues and Complements Dam Mutants in the Low Salt Environment of Escherichia Coli.” *Molecular Microbiology* 35 (5):1168–79. http://www.ncbi.nlm.nih.gov/pubmed/10712697.

Barns, S M, C F Delwiche, J D Palmer, and N R Pace. 1996. “Perspectives on Archaeal Diversity, Thermophily and Monophyly from Environmental rRNA Sequences.” *Proceedings of the National Academy of Sciences of the United States of America* 93 (17):9188–93. http://www.ncbi.nlm.nih.gov/pubmed/8799176.

Blöchl, E, R Rachel, S Burggraf, D Hafenbradl, H W Jannasch, and K O Stetter. 1997. “Pyrolobus Fumarii, Gen. and Sp. Nov., Represents a Novel Group of Archaea, Extending the Upper Temperature Limit for Life to 113 Degrees C.” *Extremophiles : Life under Extreme Conditions* 1 (1):14–21. http://www.ncbi.nlm.nih.gov/pubmed/9680332.

Boucher, Helen W, George H Talbot, Daniel K Benjamin, John Bradley, Robert J Guidos, Ronald N Jones, Barbara E Murray, et al. 2013. “10 X ’20 Progress--Development of New Drugs Active against Gram-Negative Bacilli: An Update from the Infectious Diseases Society of America.” *Clinical Infectious Diseases : An Official Publication of the Infectious Diseases Society of America* 56 (12). Oxford University Press:1685–94. https://doi.org/10.1093/cid/cit152.

Brochier-Armanet, Celine, Patrick Forterre, and Simonetta Gribaldo. 2011. “Phylogeny and Evolution of the Archaea: One Hundred Genomes Later.” *Current Opinion in Microbiology* 14 (3):274–81. https://doi.org/10.1016/j.mib.2011.04.015.

Brüssow, H, and F Desiere. 2001. “Comparative Phage Genomics and the Evolution of Siphoviridae: Insights from Dairy Phages.” *Molecular Microbiology* 39 (2):213–22. http://www.ncbi.nlm.nih.gov/pubmed/11136444.

Casjens, S., Hatfull, G., and Hendrix, R. 1992. “Evolution of dsDNA Tailed-Bacteriophage

Genomes." *Semin Virol* 3:383–97.

Cline, S W, and W F Doolittle. 1987. "Efficient Transfection of the Archaebacterium Halobacterium Halobium." *Journal of Bacteriology* 169 (3). American Society for Microbiology (ASM):1341–44. http://www.ncbi.nlm.nih.gov/pubmed/3818549.

Costa, M S da, H Santos, and E A Galinski. 1998. "An Overview of the Role and Diversity of Compatible Solutes in Bacteria and Archaea." *Advances in Biochemical Engineering/biotechnology* 61:117–53. http://www.ncbi.nlm.nih.gov/pubmed/9670799.

David Lodwick, By, Hamish N M Ross, J E F F R E Y W Almond, and A N D William D G R A N T. 1986. "Dam Methylation in the Archaebacteria." *Journal of General Microbiology* 132:3055–59. http://www.microbiologyresearch.org/docserver/fulltext/micro/132/11/mic-132-11-3055.pdf?expires=1508935066&id=id&accname=guest&checksum=C1D267413D878CC8044BD9101EEF5332.

Diaz Ricci, Juan C., and Marría Eugenia Hernández. 2000. "Plasmid Effects on *Escherichia Coli* Metabolism." *Critical Reviews in Biotechnology* 20 (2):79–108. https://doi.org/10.1080/07388550008984167.

Dyall-Smith, Mike, Sen-Lin Tang, and Carolyn Bath. 2003. "Haloarchaeal Viruses: How Diverse Are They?" *Research in Microbiology* 154 (4):309–13. https://doi.org/10.1016/S0923-2508(03)00076-7.

Fendrihan, Sergiu, Andrea Legat, Marion Pfaffenhuemer, Claudia Gruber, Gerhard Weidler, Friedrich Gerbl, and Helga Stan-Lotter. 2006. "Extremely Halophilic Archaea and the Issue of Long-Term Microbial Survival." *Re/views in Environmental Science and Bio/technology (Online)* 5 (2–3):203–18. https://doi.org/10.1007/s11157-006-0007-y.

Forterre, Patrick, Celine Brochier, and Hervé Philippe. 2002. "Evolution of the Archaea." *Theoretical Population Biology* 61 (4):409–22. http://www.ncbi.nlm.nih.gov/pubmed/12167361.

Friedman, S A, and S J Austin. 1988. "The P1 Plasmid-Partition System Synthesizes Two Essential Proteins from an Autoregulated Operon." *Plasmid* 19 (2):103–12. http://www.ncbi.nlm.nih.gov/pubmed/3420178.

Friehs, Karl. 2004. "Plasmid Copy Number and Plasmid Stability." *Advances in Biochemical Engineering/biotechnology* 86:47–82. http://www.ncbi.nlm.nih.gov/pubmed/15088763.

Gambacorta, A, A Gliozzi, and M De Rosa. 1995. "Archaeal Lipids and Their Biotechnological Applications." *World Journal of Microbiology & Biotechnology* 11 (1):115–31. https://doi.org/10.1007/BF00339140.

Gregor, Dagmar, and Felicitas Pfeifer. 2005. "In Vivo Analyses of Constitutive and Regulated Promoters in Halophilic Archaea." *Microbiology (Reading, England)* 151 (Pt 1):25–33.

https://doi.org/10.1099/mic.0.27541-0.

Gribaldo, Simonetta, and Celine Brochier-Armanet. 2006. “The Origin and Evolution of Archaea: A State of the Art.” *Philosophical Transactions of the Royal Society of London. Series B, Biological Sciences* 361 (1470). The Royal Society:1007–22. https://doi.org/10.1098/rstb.2006.1841.

Hallet, B, and D J Sherratt. 1997. “Transposition and Site-Specific Recombination: Adapting DNA Cut-and-Paste Mechanisms to a Variety of Genetic Rearrangements.” *FEMS Microbiology Reviews* 21 (2):157–78. http://www.ncbi.nlm.nih.gov/pubmed/9348666.

Happonen, Lotta Johanna, Peter Redder, Xu Peng, Laila Johanne Reigstad, David Prangishvili, and Sarah Jane Butcher. 2010. “Familial Relationships in Hyperthermo- and Acidophilic Archaeal Viruses.” *Journal of Virology* 84 (9):4747–54. https://doi.org/10.1128/JVI.02156-09.

Hayes, Christopher S, and Robert T Sauer. 2003. “Toxin-Antitoxin Pairs in Bacteria: Killers or Stress Regulators?” *Cell* 112 (1):2–4. http://www.ncbi.nlm.nih.gov/pubmed/12526786.

Hester, Christina M, and Joe Lutkenhaus. 2007. “Soj (ParA) DNA Binding Is Mediated by Conserved Arginines and Is Essential for Plasmid Segregation.” *Proceedings of the National Academy of Sciences of the United States of America* 104 (51):20326–31. https://doi.org/10.1073/pnas.0705196105.

Heuer, Holger, and Kornelia Smalla. 2012. “Plasmids Foster Diversification and Adaptation of Bacterial Populations in Soil.” *FEMS Microbiology Reviews* 36 (6):1083–1104. https://doi.org/10.1111/j.1574-6976.2012.00337.x.

Hoischen, C., Alexander Bolshoy, Kenn Gerdes, and Stephan Diekmann. 2004. “Centromere parC of Plasmid R1 Is Curved.” *Nucleic Acids Research* 32 (19):5907–15. https://doi.org/10.1093/nar/gkh920.

Holmes, M L, and M L Dyall-Smith. 1990. “A Plasmid Vector with a Selectable Marker for Halophilic Archaebacteria.” *Journal of Bacteriology* 172 (2). American Society for Microbiology (ASM):756–61. http://www.ncbi.nlm.nih.gov/pubmed/2105303.

———. 1991. “Mutations in DNA Gyrase Result in Novobiocin Resistance in Halophilic Archaebacteria.” *Journal of Bacteriology* 173 (2). American Society for Microbiology (ASM):642–48. http://www.ncbi.nlm.nih.gov/pubmed/1846146.

Huber, Harald, Michael J Hohn, Reinhard Rachel, Tanja Fuchs, Verena C Wimmer, and Karl O Stetter. 2002. “A New Phylum of Archaea Represented by a Nanosized Hyperthermophilic Symbiont.” *Nature* 417 (6884):63–67. https://doi.org/10.1038/417063a.

Iro, M, R Klein, B Gálos, U Baranyi, N Rössler, and A Witte. 2007. “The Lysogenic Region of Virus phiCh1: Identification of a Repressor-Operator System and Determination of Its Activity in Halophilic Archaea.” *Extremophiles : Life under Extreme Conditions* 11 (2):383–96.

https://doi.org/10.1007/s00792-006-0040-3.

Jarrell, Ken F, Alison D Walters, Chitvan Bochiwal, Juliet M Borgia, Thomas Dickinson, and James P J Chong. 2011. “Major Players on the Microbial Stage: Why Archaea Are Important.” *Microbiology (Reading, England)* 157 (Pt 4):919–36. https://doi.org/10.1099/mic.0.047837-0.

Jensen, R B, M Dam, and K Gerdes. 1994. “Partitioning of Plasmid R1. The parA Operon Is Autoregulated by ParR and Its Transcription Is Highly Stimulated by a Downstream Activating Element.” *Journal of Molecular Biology* 236 (5):1299–1309. http://www.ncbi.nlm.nih.gov/pubmed/8126721.

Jensen, R B, and K Gerdes. 1999. “Mechanism of DNA Segregation in Prokaryotes: ParM Partitioning Protein of Plasmid R1 Co-Localizes with Its Replicon during the Cell Cycle.” *The EMBO Journal* 18 (14). European Molecular Biology Organization:4076–84. https://doi.org/10.1093/emboj/18.14.4076.

Kaiser, Gary. 2017. “No Title.” 2017. https://bio.libretexts.org/TextMaps/Map:_Microbiology_(Kaiser)/Unit_1:_Introduction_to_Microbiology_and_Prokaryotic_Cell_Anatomy/1:_Fundamentals_of_Microbiology/1.3:_Classification_-_The_Three_Domain_System.

Kamekura, M., M. L. Dyall-Smith, V. Upasani, A. Ventosa, and M. Kates. 1997. “Diversity of Alkaliphilic Halobacteria: Proposals for Transfer of Natronobacterium Vacuolatum, Natronobacterium Magadii, and Natronobacterium Pharaonis to Halorubrum, Natrialba, and Natronomonas Gen. Nov., Respectively, as Halorubrum Vacuolatum Comb. Nov., Natrialba Magadii Comb. Nov., and Natronomonas Pharaonis Comb. Nov., Respectively.” *International Journal of Systematic Bacteriology* 47 (3):853–57. https://doi.org/10.1099/00207713-47-3-853.

Klein, R, U Baranyi, N Rössler, B Greineder, H Scholz, and A Witte. 2002. “Natrialba Magadii Virus phiCh1: First Complete Nucleotide Sequence and Functional Organization of a Virus Infecting a Haloalkaliphilic Archaeon.” *Molecular Microbiology* 45 (3):851–63. http://www.ncbi.nlm.nih.gov/pubmed/12139629.

Klingl, Andreas. 2014. “S-Layer and Cytoplasmic Membrane - Exceptions from the Typical Archaeal Cell Wall with a Focus on Double Membranes.” *Frontiers in Microbiology* 5 (November):624. https://doi.org/10.3389/fmicb.2014.00624.

Lam, W L, and W F Doolittle. 1992. “Mevinolin-Resistant Mutations Identify a Promoter and the Gene for a Eukaryote-like 3-Hydroxy-3-Methylglutaryl-Coenzyme A Reductase in the Archaebacterium Haloferax Volcanii.” *The Journal of Biological Chemistry* 267 (9):5829–34. http://www.ncbi.nlm.nih.gov/pubmed/1556098.

Landy, A. 1989. “Dynamic, Structural, and Regulatory Aspects of Lambda Site-Specific Recombination.” *Annual Review of Biochemistry* 58 (1):913–41. https://doi.org/10.1146/annurev.bi.58.070189.004405.

Lanyi, J K. 1974. “Salt-Dependent Properties of Proteins from Extremely Halophilic Bacteria.” *Bacteriological Reviews* 38 (3). American Society for Microbiology (ASM):272–90. http://www.ncbi.nlm.nih.gov/pubmed/4607500.

Lanyi, Janos K. 1995. “Bacteriorhodopsin as a Model for Proton Pumps.” *Nature* 375 (6531):461–63. https://doi.org/10.1038/375461a0.

Large, Andrew, Claudia Stamme, Christian Lange, Zhenhong Duan, Thorsten Allers, Jörg Soppa, and Peter A Lund. 2007. “Characterization of a Tightly Controlled Promoter of the Halophilic Archaeon Haloferax Volcanii and Its Use in the Analysis of the Essential cct1 Gene.” *Molecular Microbiology* 66 (5):1092–1106. https://doi.org/10.1111/j.1365-2958.2007.05980.x.

Leplae, Raphaël, Gipsi Lima-Mendez, and Ariane Toussaint. 2006. “A First Global Analysis of Plasmid Encoded Proteins in the ACLAME Database.” *FEMS Microbiology Reviews* 30 (6):980–94. https://doi.org/10.1111/j.1574-6976.2006.00044.x.

Ma, Yanhe, Erwin A Galinski, William D Grant, Aharon Oren, and Antonio Ventosa. 2010. “Halophiles 2010: Life in Saline Environments.” *Applied and Environmental Microbiology* 76 (21). American Society for Microbiology (ASM):6971–81. https://doi.org/10.1128/AEM.01868-10.

Margesin, R, and F Schinner. 2001. “Potential of Halotolerant and Halophilic Microorganisms for Biotechnology.” *Extremophiles : Life under Extreme Conditions* 5 (2):73–83. http://www.ncbi.nlm.nih.gov/pubmed/11354458.

Mayrhofer-Iro, M., A. Ladurner, C. Meissner, C. Derntl, M. Reiter, F. Haider, K. Dimmel, et al. 2013. “Utilization of Virus Ch1 Elements To Establish a Shuttle Vector System for Halo(alkali)philic Archaea via Transformation of Natrialba Magadii.” *Applied and Environmental Microbiology* 79 (8):2741–48. https://doi.org/10.1128/AEM.03287-12.

Million-Weaver, Samuel, and Manel Camps. 2014. “Mechanisms of Plasmid Segregation: Have Multicopy Plasmids Been Overlooked?” *Plasmid* 75 (September). NIH Public Access:27–36. https://doi.org/10.1016/j.plasmid.2014.07.002.

Mochizuki, Tomohiro, Mart Krupovic, Gérard Pehau-Arnaudet, Yoshihiko Sako, Patrick Forterre, and David Prangishvili. 2012. “Archaeal Virus with Exceptional Virion Architecture and the Largest Single-Stranded DNA Genome.” *Proceedings of the National Academy of Sciences of the United States of America* 109 (33). National Academy of Sciences:13386–91. https://doi.org/10.1073/pnas.1203668109.

Murray, Heath, and Jeff Errington. 2008. “Dynamic Control of the DNA Replication Initiation Protein DnaA by Soj/ParA.” *Cell* 135 (1):74–84. https://doi.org/10.1016/j.cell.2008.07.044.

Nayek, Arnab, Parth Sarthi Sen Gupta, Shyamashree Banerjee, Buddhadev Mondal, and Amal K Bandyopadhyay. 2014. “Salt-Bridge Energetics in Halophilic Proteins.” Edited by Eugene A. Permyakov. *PloS One* 9 (4):e93862. https://doi.org/10.1371/journal.pone.0093862.

Ng, W L, and S DasSarma. 1993. “Minimal Replication Origin of the 200-Kilobase Halobacterium Plasmid pNRC100.” *Journal of Bacteriology* 175 (15):4584–96. http://www.ncbi.nlm.nih.gov/pubmed/8335618.

Norris, P R, N P Burton, and N A Foulis. 2000. “Acidophiles in Bioreactor Mineral Processing.” *Extremophiles : Life under Extreme Conditions* 4 (2):71–76. http://www.ncbi.nlm.nih.gov/pubmed/10805560.

Oren, A. 1999. “Bioenergetic Aspects of Halophilism.” *Microbiology and Molecular Biology Reviews : MMBR* 63 (2):334–48. http://www.ncbi.nlm.nih.gov/pubmed/10357854.

Oren, A, G Bratbak, and M Heldal. 1997. “Occurrence of Virus-like Particles in the Dead Sea.” *Extremophiles : Life under Extreme Conditions* 1 (3):143–49. http://www.ncbi.nlm.nih.gov/pubmed/9680320.

Oren, Aharon. 2002. “Molecular Ecology of Extremely Halophilic Archaea and Bacteria.” *FEMS Microbiology Ecology* 39 (1):1–7. https://doi.org/10.1111/j.1574-6941.2002.tb00900.x.

Ozyamak, Ertan, Justin M. Kollman, and Arash Komeili. 2013. “Bacterial Actins and Their Diversity.” *Biochemistry* 52 (40):6928–39. https://doi.org/10.1021/bi4010792.

Patenge, N, A Haase, H Bolhuis, and D Oesterhelt. 2000. “The Gene for a Halophilic Beta-Galactosidase (bgaH) of Haloferax Alicantei as a Reporter Gene for Promoter Analyses in Halobacterium Salinarum.” *Molecular Microbiology* 36 (1):105–13. http://www.ncbi.nlm.nih.gov/pubmed/10760167.

Paunesku, T., S. Mittal, M. Protić, J. Oryhon, S. V. Korolev, A. Joachimiak, and G. E. Woloschak. 2001. “Proliferating Cell Nuclear Antigen (PCNA): Ringmaster of the Genome.” *International Journal of Radiation Biology* 77 (10). Taylor & Francis:1007–21. https://doi.org/10.1080/09553000110069335.

Pester, Michael, Christa Schleper, and Michael Wagner. 2011. “The Thaumarchaeota: An Emerging View of Their Phylogeny and Ecophysiology.” *Current Opinion in Microbiology* 14 (3):300–306. https://doi.org/10.1016/j.mib.2011.04.007.

Prangishvili, David, Patrick Forterre, and Roger A. Garrett. 2006. “Viruses of the Archaea: A Unifying View.” *Nature Reviews Microbiology* 4 (11):837–48. https://doi.org/10.1038/nrmicro1527.

Reed, Christopher J., Hunter Lewis, Eric Trejo, Vern Winston, and Caryn Evilia. 2013. “Protein Adaptations in Archaeal Extremophiles.” *Archaea* 2013:1–14. https://doi.org/10.1155/2013/373275.

Reiter, Michael. 2010. “Gene Regulation of ϕCh1.”

Rice, G, K Stedman, J Snyder, B Wiedenheft, D Willits, S Brumfield, T McDermott, and M J Young. 2001. “Viruses from Extreme Thermal Environments.” *Proceedings of the National Academy of Sciences of the United States of America* 98 (23). National Academy of

Sciences:13341–45. https://doi.org/10.1073/pnas.231170198.

Sauer, T, and E A Galinski. 1998. “Bacterial Milking: A Novel Bioprocess for Production of Compatible Solutes.” *Biotechnology and Bioengineering* 57 (3):306–13. http://www.ncbi.nlm.nih.gov/pubmed/10099207.

Schiraldi, Chiara, Mariateresa Giuliano, and Mario De Rosa. 2002. “Perspectives on Biotechnological Applications of Archaea.” *Archaea* 1 (2). Hindawi:75–86. https://doi.org/10.1155/2002/436561.

Schnabel, Heinke, and Wolfram Zillig. 1984. “Circular Structure of the Genome of Phage ?H in a Lysogenic Halobacterium Halobium.” *MGG Molecular & General Genetics* 193 (3). Springer-Verlag:422–26. https://doi.org/10.1007/BF00382078.

Schumacher, K, E Heine, and H Höcker. 2001. “Extremozymes for Improving Wool Properties.” *Journal of Biotechnology* 89 (2–3):281–88. http://www.ncbi.nlm.nih.gov/pubmed/11500223.

Shahmohammadi, H R, E Asgarani, H Terato, T Saito, Y Ohyama, K Gekko, O Yamamoto, and H Ide. 1998. “Protective Roles of Bacterioruberin and Intracellular KCl in the Resistance of Halobacterium Salinarium against DNA-Damaging Agents.” *Journal of Radiation Research* 39 (4):251–62. http://www.ncbi.nlm.nih.gov/pubmed/10196780.

Silva, Filomena, João A. Queiroz, and Fernanda C. Domingues. 2012. “Evaluating Metabolic Stress and Plasmid Stability in Plasmid DNA Production by Escherichia Coli.” *Biotechnology Advances* 30 (3):691–708. https://doi.org/10.1016/j.biotechadv.2011.12.005.

Snyder, Jamie C, Kenneth Stedman, George Rice, Blake Wiedenheft, Josh Spuhler, and Mark J Young. 2003. “Viruses of Hyperthermophilic Archaea.” *Research in Microbiology* 154 (7):474–82. https://doi.org/10.1016/S0923-2508(03)00127-X.

Spang, Anja, Roland Hatzenpichler, Céline Brochier-Armanet, Thomas Rattei, Patrick Tischler, Eva Spieck, Wolfgang Streit, David A Stahl, Michael Wagner, and Christa Schleper. 2010. “Distinct Gene Set in Two Different Lineages of Ammonia-Oxidizing Archaea Supports the Phylum Thaumarchaeota.” *Trends in Microbiology* 18 (8):331–40. https://doi.org/10.1016/j.tim.2010.06.003.

Stieber, Daniel, Philippe Gabant, and Cédric Szpirer. 2008. “The Art of Selective Killing: Plasmid Toxin/antitoxin Systems and Their Technological Applications.” *BioTechniques* 45 (3):344–46. https://doi.org/10.2144/000112955.

Svoboda, Tatjana. 2011. “Characterization of Putative Repressors of the Temperate Phage ϕCh1 and Analysis of the Flagellum Operon as a Putative Receptor of ϕCh1.”

Tadeo, Xavier, Blanca López-Méndez, Tamara Trigueros, Ana Laín, David Castaño, and Oscar Millet. 2009. “Structural Basis for the Aminoacid Composition of Proteins from Halophilic Archea.” Edited by Gregory A. Petsko. *PLoS Biology* 7 (12):e1000257.

https://doi.org/10.1371/journal.pbio.1000257.

Tenchov, Boris, Erin M Vescio, G Dennis Sprott, Mark L Zeidel, and John C Mathai. 2006. “Salt Tolerance of Archaeal Extremely Halophilic Lipid Membranes.” *The Journal of Biological Chemistry* 281 (15):10016–23. https://doi.org/10.1074/jbc.M600369200.

Tindall et al. 1984. “Natronobacterium Gen. Nov. and Natronococcus Gen. Nov., Two New Genera of Haloalkaliphilic Archaebacteria.” *Systematic and Applied Microbiology* 5:41–57.

Vossenberg, J L van de, A J Driessen, and W N Konings. 1998. “The Essence of Being Extremophilic: The Role of the Unique Archaeal Membrane Lipids.” *Extremophiles : Life under Extreme Conditions* 2 (3):163–70. http://www.ncbi.nlm.nih.gov/pubmed/9783161.

Witte, A, U Baranyi, R Klein, M Sulzner, C Luo, G Wanner, D H Krüger, and W Lubitz. 1997. “Characterization of Natronobacterium Magadii Phage Phi Ch1, a Unique Archaeal Phage Containing DNA and RNA.” *Molecular Microbiology* 23 (3):603–16. http://www.ncbi.nlm.nih.gov/pubmed/9044293.

Woese, C R, and G E Fox. 1977. “Phylogenetic Structure of the Prokaryotic Domain: The Primary Kingdoms.” *Proceedings of the National Academy of Sciences of the United States of America* 74 (11):5088–90. http://www.ncbi.nlm.nih.gov/pubmed/270744.

Woese, C R, O Kandler, and M L Wheelis. 1990. “Towards a Natural System of Organisms: Proposal for the Domains Archaea, Bacteria, and Eucarya.” *Proceedings of the National Academy of Sciences of the United States of America* 87 (12):4576–79. http://www.ncbi.nlm.nih.gov/pubmed/2112744.

Zhou, Meixian, Hua Xiang, Chaomin Sun, and Huarong Tan. 2004. “Construction of a Novel Shuttle Vector Based on an RCR-Plasmid from a Haloalkaliphilic Archaeon and Transformation into Other Haloarchaea.” *Biotechnology Letters* 26 (14):1107–13. https://doi.org/10.1023/B:BILE.0000035493.21986.20.

Zuckerkandl, E, and L Pauling. 1965. “Molecules as Documents of Evolutionary History.” *Journal of Theoretical Biology* 8 (2):357–66. http://www.ncbi.nlm.nih.gov/pubmed/5876245.

5. Abstract

ϕCh1 is a temperate virus which infects the haloalkaliphilic archaeon *Natrialba magadii*. Investigating the viral transcriptional regulation is of key importance to understand regulation of its life cycle which further contributes to development of tools for genetic manipulation on the host's level. ϕCh1 contains 98 open reading frames (ORFs). This study focused on characterization of two ORFs: ORF46 and ORF49.

For elucidation of ORF46 and ORF49, deletion mutant strains lacking these ORFs were constructed, in which the novobiocin resistance cassette replaced ORF46 and ORF49 by homologous recombination. Successful homologous recombination was confirmed with analytical PCRs and Southern blot for ORF46 enabling detection of specific DNA sequences. Further characterization of deletion mutant strains included the growth kinetics analysis, evaluation of number of reduced virus particles performed with virus titer analysis as well as expression of specific proteins which were detected by Western blot.

ORF46 encodes Soj protein which is involved in partitioning of plasmid as described by previous studies. This study showed that deletion of ORF46 results in an earlier onset of lysis of *N. magadii* L11-ΔORF46(*soj*)-NovR-R. However, no reduction in the number of released virus particles could be detected. In addition, Western blot detecting the Soj protein did not show its presence in the *N. magadii* L11-ΔORF46(*soj*)-NovR-R. However, the expression of ORF11 which encodes the major capsid protein E was detected on the same day when lysis occurred in both strains. ORF11 expression decreases over time in deletion mutant strain. Second part of this work focused on identifying and elucidation of elements shown to be important for viral switch between lytic and lysogenic life cycle. A study in 2007 revealed ORF49 by analyzing the mutant ϕCh1-1 which phenotype yielded larger plaques and an earlier onset of lysis of the host *N. magadii*. Therefore, ϕCh1 ORF49 deletion mutant was constructed in order to characterize its function. Earlier onset of lysis in the absence of ORF49 was confirmed. Expression of ORF11 was detected one day earlier in the deletion mutant strain. However, ORF11 expression increased

over time in the wild type *N. magadii* L11 whereas its reduction was observed in the deletion mutant strain.

Expression patterns of another genes, e.g. ORF34 and methyltransferase gene which are located in the central part and at the 3' end of ϕCh1 in the deletion mutant strains, still remain unknown. Therefore, it would be of key importance to perform Western Blot analyses in the future to see the expression of the mentioned genes.

6. Zusammenfassung

ϕCh1 ist ein temperenter Virus, dass das haloalkaliphile Archeon *Natrialba magadii* infiziert. Die Erforschung der viralen transkriptionellen Regulation ist zum Verständnis der Regulation des Lebenszyklus des Archeon von großer Bedeutung, denn diese kann im Weiteren zur Entwicklung von Methoden zur genetische Manipulation der Zielzelle beitragen. ϕCh1 beinhaltet insgesamt 98 offene Leserrahmen (ORFs); diese Studie konzentriert sich auf die Charakterisierung von zwei ORFs, ORF46 und ORF49.

Zur Erforschung von ORF46 und ORF49 wurden deletionsmutierte hergestellt, in denen eine Novobiocin-Resistänz Kassette die ORFs mittels homologer Rekombination ersetzt. Die erfolgreiche homologe Rekombination wurde mittels analytischer PCRs und Southern Blots zur Detektion von ORF46-spezifischer DNA-Sequenzen bestätigt. Eine weitere Charakterisierung der deletionsmutierten Stämme erfolgte mittels Analyse von Wachstumskinetik, Quantifizierung reduzierter Viruspartikel mittels Virus-Titer-Analyse und Expression spezifischer Proteine mittels Western Blot.

ORF46 exprimiert das Soj-Protein, das, wie in früheren Studien gezeigt wurde, in der Partitionierung von Plasmiden involviert ist. In dieser Studie konnte gezeigt werden, dass die Deletion von ORF46 zur einem früheren Beginn der Lyse von *N. magadii* L11 ΔORF46(*soj*)-NovR-R führt. Es konnte jedoch weder eine Reduktion der freigesetzten Viruspartikel gemessen, noch Soj-Protein mittels Western Blot in *N. magadii* L11 ΔORF46(*soj*)-NovR-R nachgewiesen werden.

Dafür konnte die Expression von ORF11, dass das major capsid protein E exprimiert, in beiden Stämmen am Tag des Lysebeginns detektiert werden. Die Expression von ORF11 zeigte sich im zeitlichen Verlauf in den deletionsmutierten Stämmen rückläufig.

Der zweite Teil der Arbeit fokussierte sich auf Identifizierung und Erforschung von Elementen, die eine bedeutende Rolle im viralen Umschaltemechanismus von einem lytischen auf einen lysogenen Lebenszyklus spielen. Eine 2007 publizierte Studie entdeckte ORF46 bei der Erforschung einer ϕCh1-1-Mutante, deren Phänotyp durch größere Plaques und einen früheren Lysebeginn der Zielzelle *N. magadii* auffiel. Daraufhin wurde eine ϕCh1 ORF49-Deletionsmutante konstruiert, um deren Funktion zu charakterisieren. Ein früherer Lysebeginn in der Abwesenheit von ORF49 konnte bestätigt werden. Die Expression von ORF11 konnte einen Tag früher in den deletionsmutierten Stämmen nachgewiesen werden. Die Expression nahm mit der Zeit im Wildtyp *N. magadii* L11 zu, während er in der Deletionsmutante abnahm.

Die Expressionsmechanismen anderer Gene, z.B. von ORF34 und Methyltransferase-Genen, die in der Deletionsmutante im Zentrum und am 3‘-Ende von ϕCh1 lokalisiert sind, bleiben weiterhin unbekannt. Die Erforschung der Expression dieser Gene mittels Western Blot wird in Zukunft eine bedeutende Rolle spielen.